UNCLASSIFIED

AD 274 150

Reproduced
by the

ARMED SERVICES TECHNICAL INFORMATION AGENCY
ARLINGTON HALL STATION
ARLINGTON 12, VIRGINIA

UNCLASSIFIED

NOTICE: When government or other drawings, specifications or other data are used for any purpose other than in connection with a definitely related government procurement operation, the U. S. Government thereby incurs no responsibility, nor any obligation whatsoever; and the fact that the Government may have formulated, furnished, or in any way supplied the said drawings, specifications, or other data is not to be regarded by implication or otherwise as in any manner licensing the holder or any other person or corporation, or conveying any rights or permission to manufacture, use or sell any patented invention that may in any way be related thereto.

274 150

274 150

RADC-TDR-61-285
ASTIA Document No. AD-

BISTATIC CROSS SECTIONS OF CYLINDRICAL WIRES

J. T. deBettencourt

PICKARD & BURNS, INC.
103 Fourth Avenue
Waltham 54, Massachusetts

Subsidiary Of

GORHAM CORPORATION

ASTIA

Scientific Report No. 1

Contract No. AF30(602)-2412

Prepared For

ROME AIR DEVELOPMENT CENTER
Air Research and Development Command
United States Air Force
Griffiss Air Force Base
New York

P&B Pub. No. 735A

Copy No. 17

RADC-TDR-61-285
ASTIA Document No. AD-

BISTATIC CROSS SECTIONS OF CYLINDRICAL WIRES

J. T. deBettencourt

PICKARD & BURNS, INC.
10.3 Fourth Avenue
Waltham 54, Massachusetts

Subsidiary Of

GORHAM CORPORATION

Scientific Report No. 1

Contract No. AF30(602)-2412

Prepared For

ROME AIR DEVELOPMENT CENTER
Air Research and Development Command
United States Air Force
Griffiss Air Force Base
New York

P&B Pub. No. 735A

Copy No. 27

Qualified requestors may obtain copies of this report from the ASTIA Document Service Center, Dayton 2, Ohio. ASTIA Services for the Department of Defense contractors are available through the "Field of Interest Register" on a "need-to-know" certified by the cognizant military agency of their project or contract.

FOREWORD

This investigation was supported in part by Air Force Cambridge Research Laboratories through Contract AF19(604)-8341 with Pickard & Burns, Inc.

Patricia Concannon developed the digital computer program and obtained and plotted the data for the figures.

ABSTRACT

Bistatic scattering cross sections of a thin, perfectly conducting cylinder are developed using the variational method. This method was used by Tai[1] for obtaining monostatic (back scatter) radar cross sections. Resulting expressions are developed for wires of 3/2 λ_o length or less, where λ_o is the free space wavelength. The wires are assumed to be in air or vacuo.

The resulting calculations apply to the case where the incident electric vector lies in the incident plane and the receiving antenna is polarized parallel to the scattering plane.

Curves are plotted for σ_{MS}/λ_o^2 vs θ_o where σ_{MS} is the monostatic scattering cross section in the same units as λ_o^2, for various values of $2h/\lambda_o$ in the range $0.5 \leq 2h/\lambda_o \leq 1.5$ for a thickness parameter $\Omega = 2 \log_e 2h/a = 10$ and 13.6. The wire length and radius are 2h and a, respectively. θ_o is the angle of incidence (and back scattering) with respect to the wire. Results for monostatic cross sections agree with those of others for their values of Ω and $2h/\lambda_o$.

For bistatic cross sections σ_{BS}, curves are given for σ_{BS}/λ_o^2 vs θ for $\Omega = 10$, in the range $0.5 \leq 2h/\lambda_o \leq 1.5$, with θ_o as the parameter. θ is the scattering or reflection angle with respect to the wire.

The curves for bistatic scattering show aspect and frequency sensitivity. Double humps or lobes are generally asymmetric in θ for given values of θ_o and particularly for wire lengths greater than 0.75 λ_o.

Thus "forward scattering" gives larger cross sections than back scattering under certain combinations of θ_o and $2h/\lambda_o$.

If the incident wave from a transmitter is polarized such that ψ_T is the polarizing angle of the incident electric vector with respect to the plane of incidence, the curves can be used by multiplying σ / λ_o^2 by $\cos^2 \psi_T$. If, in addition, the receiver is polarized at an angle ψ_R with respect to the scattering or reflection plane, the values of σ / λ_o^2 should be multiplied by $(\cos^2 \psi_T \cos^2 \psi_R)$.

Application of the curves of σ / λ_o^2 to determination of total transmission losses in a bistatic system are discussed, with a sample calculation.

TABLE OF CONTENTS

LIST OF ILLUSTRATIONS

LIST OF ILLUSTRATIONS (Continued)

BISTATIC CROSS SECTIONS OF CYLINDRICAL WIRES

I. INTRODUCTION

For a certain radio echo propagation problem it was required to investigate optimum locations of a transmitter and receiver with respect to a scattering source assumed to be a cylindrical parasitic wire of length less than a couple of wavelengths. Of particular interest was the case of separated transmitter and receiver, giving rise to bistatic scattering, as opposed to the usual radar back scatter, or monostatic radar, case. The problem thus involves the determination of the scattering cross section of the wire, its aspect sensitivity and frequency-dependence.

For radar or monostatic back scattering, several analytic methods have been employed to determine the back scatter cross section. These include the e.m.f. method, iteration method, and use of the variational principle. The methods and results are reviewed in texts by King[2], Mentzer[3] and King and Wu[4], with references to the original work. For convenience we shall use the variational principle as applied by Tai[1] for back scatter cross sections, but then extend the development to bistatic arrangements.

The assumptions regarding the scattering model used here for a free space wavelength λ_o, are that the cylindrical wire of length $2h$ and radius a is not too thick and can be described by a thickness parameter $\Omega = 2 \log_e 2h/a$, that $2h/\lambda_o \leq 1.5$ and that the wire has infinite

conductivity. At a later time the effect of finite conductivity can be determined by assuming that such effect is ascribable to an internal impedance-per-unit-length term included in the expressions for current, as was done by Cassedy and Fainberg[5] for back scatter cross sections. The impedance per unit length z_i depends upon conductivity and dielectric constant of the wire.

In Section II the expressions of Tai[1] using the variational principle are reviewed. (Certain typographical errors in his text are mentioned, the details being delineated in the Appendix.) Computations using the corrected expressions were made for monostatic radar cross sections for $\Omega = 10$ and 13.6. Curves of σ / λ_o^2 vs θ_o agree with those of others[1], [2], [3], [4] for given values of $2h/\lambda_o$. Additional values of cross sections are also plotted for other values of $2h/\lambda_o$.

In Section III expressions are developed for bistatic cross sections, σ_{BS}. Values of σ_{BS} in square wavelengths are computed for $\Omega = 10$. Curves are plotted showing the variation of σ_{BS}/λ_o^2 vs scatter (or reflection) angle θ for various incident angles θ_o. The polarizing angle ψ_T of the incident field from a transmitter is assumed zero, i.e. the incident field lies in the plane containing the wire and direction of wave propagation and reflection. Values are given for $2h/\lambda_o = 0.5$, 0.75, 1.0, 1.25 and 1.5. Where $\theta = \theta_o$ the curves become those for the back scattering case of Section II.

Section IV contains the development of expressions for the current distributions. Curves are presented in normalized form for the

case of $2h = \lambda_o/2$ and $2h = \lambda_o$ in an attempt to understand the lobe phenomena in the scattered field, by the "forced" and "resonant" current contributions to total current.

The use of these curves can be extended to those cases when the incident electric field and the receiver antenna polarization are not parallel to the incident or scattering planes. If ψ_T is the angle of incident electric vector direction (polarization) with respect to the incident plane, the curves for σ/λ_o^2 should be multiplied by $\cos^2 \psi_T$. If, additionally, the receiver antenna electric polarization is described by an angle ψ_R with respect to the scattering plane, then the values of σ/λ_o^2 should be multiplied by $(\cos^2 \psi_T \cos^2 \psi_R)$.

A discussion of the application of the curves of σ/λ_o^2 is contained in Section V, with reference to total transmission losses for bistatic scattering as determined from the transmission equation.

II. MONOSTATIC (RADAR) CROSS SECTIONS - VARIATIONAL EXPRESSIONS OF TAI

Consider a wave incident upon a cylindrical wire of length 2h, radius a, such that $\Omega = 2 \log_e 2h/a$ and the geometry of the situation is as in Figure 1. The angle of incidence is θ_o measured between the wire-axis (Z-axis) and the direction of incidence. The incident electric vector E_i is a complex vector denoted by $\underset{\sim}{\bar{E}}_i$ (tilde represents complex quantity, bar represents vector quantity). This vector is polarized at an angle ψ between its direction in space and the plane containing the direction of incidence and wire axis.

For the radar back scattering case, the scattered field component of interest is that scattered back along the direction θ_o towards the transmitter and received by a receiver located coincident with the transmitter. It is assumed that the wire is in the far-field of the transmitter and that the receiver antenna is in the far-field of that scattered by the wire. Hence the only components of interest are those perpendicular to the direction of propagation, or θ_o components in Figure 1.

Let E_i be the magnitude $\left| \underset{\sim}{\bar{E}}_i \right|$, i.e. peak value in time. The current induced in the wire is then proportional to $E_i \cos\psi \sin\theta_o$. The development from here follows Tai[1]. The first-order trial function for the distribution of the current I_z is assumed to be of the form:

$$I(z) = I_o \left[f_c(z) + A f_s(z) \right] \qquad (1)$$

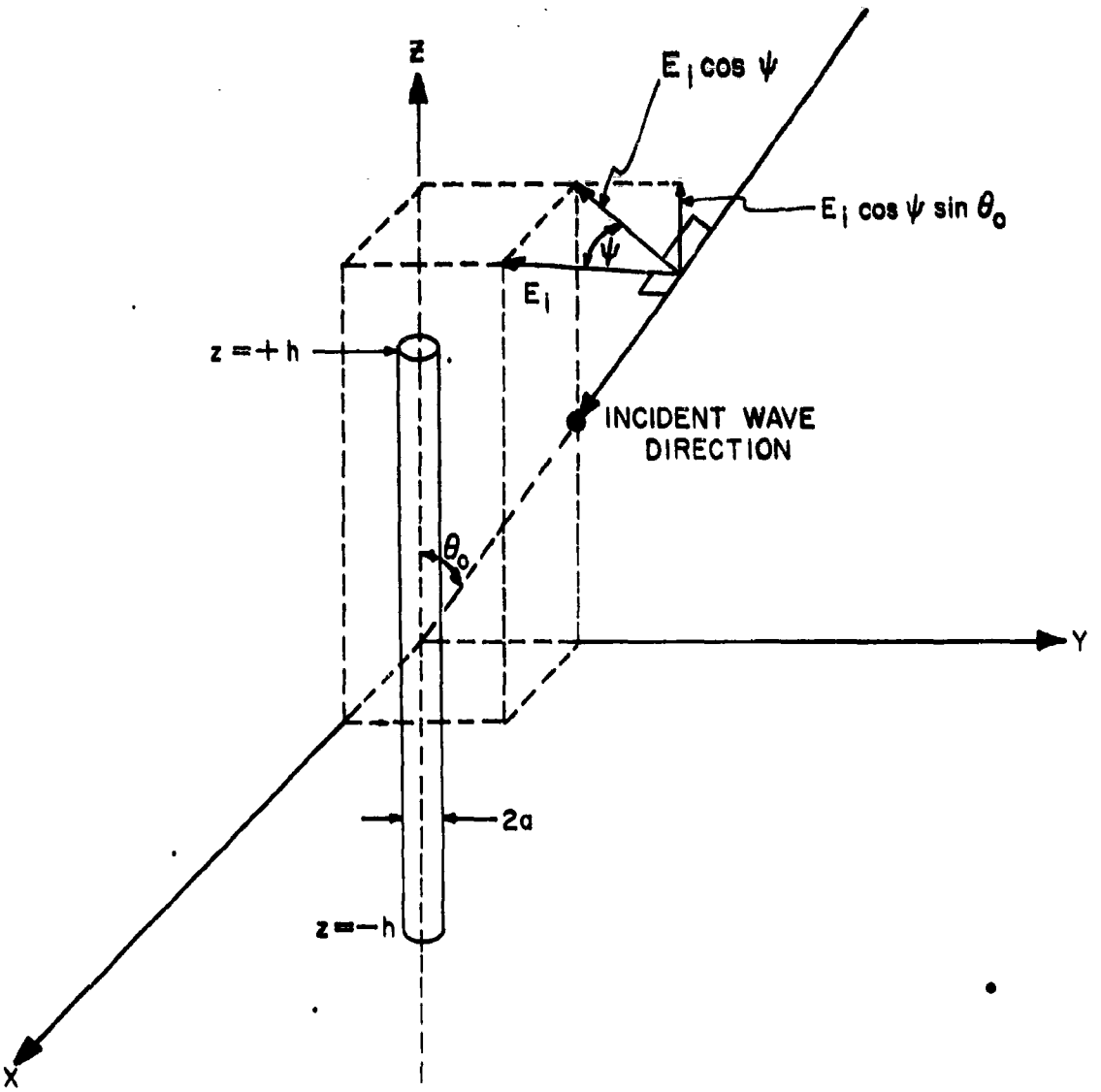

FIGURE 1. GEOMETRY OF INCIDENT ELECTRIC WAVE VECTOR AND WIRE SCATTERER

where

$$\left.\begin{aligned} f_c(z) &= \cos \beta_o z \cos(\beta_o h \cos\theta_o) - \cos \beta_o h \cos(\beta_o z \cos\theta_o) \\ f_s(z) &= \sin \beta_o z \sin(\beta_o h \cos\theta_o) - \sin \beta_o h \sin(\beta_o z \cos\theta_o) \end{aligned}\right\} \quad (2)$$

with

$$\beta_o = 2\pi / \lambda_o$$

and where I_o and A are constants. (Tai evaluates A and we shall find it useful to evaluate I_o to obtain "forced" and "resonant" components of I(z) distribution.)

Tai[1] obtains the back scattering cross section for the monostatic radar case as

$$\sigma_{MS}(\theta_o, \psi) = \frac{4\pi \cos^4\psi}{\beta_o^2} \left|S\right|^2 = \frac{\lambda_o^2}{\pi} \cos^4\psi \left|S\right|^2. \quad (3)$$

(This is Tai's $\sigma(\theta, \psi)$ in his equation (10), and we use β_o for his k.) The quantity S of Tai's is complex and may be considered as a "scattering coefficient", being independent of ψ.

By averaging over all values of ψ, Tai obtains an average cross section

$$\overline{\sigma_{MS}(\theta_o)} = \overline{\sigma_{MS}(\theta_o, \psi)} = \frac{3}{8\pi} \lambda_o^2 \left|S\right|^2. \quad (4)$$

(This is Tai's $\sigma(\theta)$ in his equation (12); we are interested in (3) rather than (4).)

When $\psi = 0$

$$\sigma_{MS}(\theta_o, \psi = 0) = \frac{\lambda_o^2}{\pi} \left|S\right|^2. \quad (5)$$

The constant A in (1) is given by Tai[1] as

$$A = \frac{g_s \gamma_c}{g_c \gamma_s} \tag{6}$$

and S becomes

$$S = \frac{g_c^2}{\gamma_c} + \frac{g_s^2}{\gamma_s} \tag{7}$$

The quantity g_c is real, g_s imaginary, and γ_c and γ_s are complex integrals:

$$g_c = \beta_o \sin\theta_o \int_{-h}^{h} f_c(z)\, e^{j\beta_o z \cos\theta_o}\, dz \tag{8a}$$

$$g_s = \beta_o \sin\theta_o \int_{-h}^{h} f_s(z)\, e^{j\beta_o z \cos\theta_o}\, dz \tag{8b}$$

$$\gamma_c = j \int_{-h}^{h} \int_{-h}^{h} f_c(z)\, f_c(z')\, K(z-z')\, dz\, dz' \tag{8c}$$

$$\gamma_s = j \int_{-h}^{h} \int_{-h}^{h} f_s(z)\, f_s(z')\, K(z-z')\, dz\, dz' \tag{8d}$$

with the kernel $K(z-z')$ being given by

$$K(z-z') = \beta_o \left(1 + \frac{1}{\beta_o^2} \frac{\partial^2}{\partial z^2}\right) \frac{e^{-j\beta_o R}}{R} \tag{9}$$

$$R = \left[(z-z')^2 + a^2\right]^{1/2}$$

The evaluation of the integrals (8) is given in Appendix A. Typographical errors in the printed version of Tai's paper occur in his evaluation of (8b), (8c) and (8d), i.e. in his equations (Appendix) (3)

in which a "cos x" should be "sin x", his equation (6) should contain a term "$\cos^2$ qxL (4x)" and his equation (7) should contain a term "$\sin^2$ qxL (4x)". The symbols are explained in Appendix A.

With these corrections, values of the average cross section, given by (4), were computed using an IBM 1620 computer for 2h/a = 900, Ω = 13.6, and $2h/\lambda_o$ = 0.5, 1.5 and 2.0. (The results compare almost exactly with Tai's curves Figures 2, 3, and 4, so that his results are satisfactory but the printed equations need the corrections aforementioned.)

Curves for the average cross section (i.e. Tai's $\sigma(\theta)/\lambda^2$) $\sigma_{MS}(\theta_o)/\lambda_o^2$ vs θ_o for Ω = 13.6 (2h/a = 900) are shown in Figures 2, 3, and 4 for $2h/\lambda_o$ = 0.5, 0.75 and 1.5 respectively; Figures 2 and 4 being the same as those of Tai[1], King[2], King and Wu[4] and Mentzer[3].

For a thicker antenna for which 2h/a = 150, Ω = 10 similar curves are given in Figures 5 through 10 for $2h/\lambda_o$ = 0.5, 0.75, 0.80, 0.90, 1.0, and 1.25 respectively. A polar plot for $2h/\lambda_o$ = 1.5 is shown in Figure 11 for Ω = 13.6 corresponding to Figure 4.

The small integral values chosen (for Ω = 10) between $2h/\lambda_o$ = 0.75 and 1.25 were an attempt to depict the "double hump" development shown previously at $2h/\lambda_o$ = 0.10. With $2h/\lambda_o$, a single broad peak is noted. At $2h/\lambda_o$ = 0.80 a minor double hump begins to appear, being better developed at 0.90. The two peaks are well developed in the case $2h/\lambda_o$ = 1.0, but a minor lobe appears at broadside (θ_o = 90°) incidence in Figure 9. Assymetry appears in the major lobes at $2h/\lambda_o$ = 1.25 in Figure 10. The lobes appear to separate further as

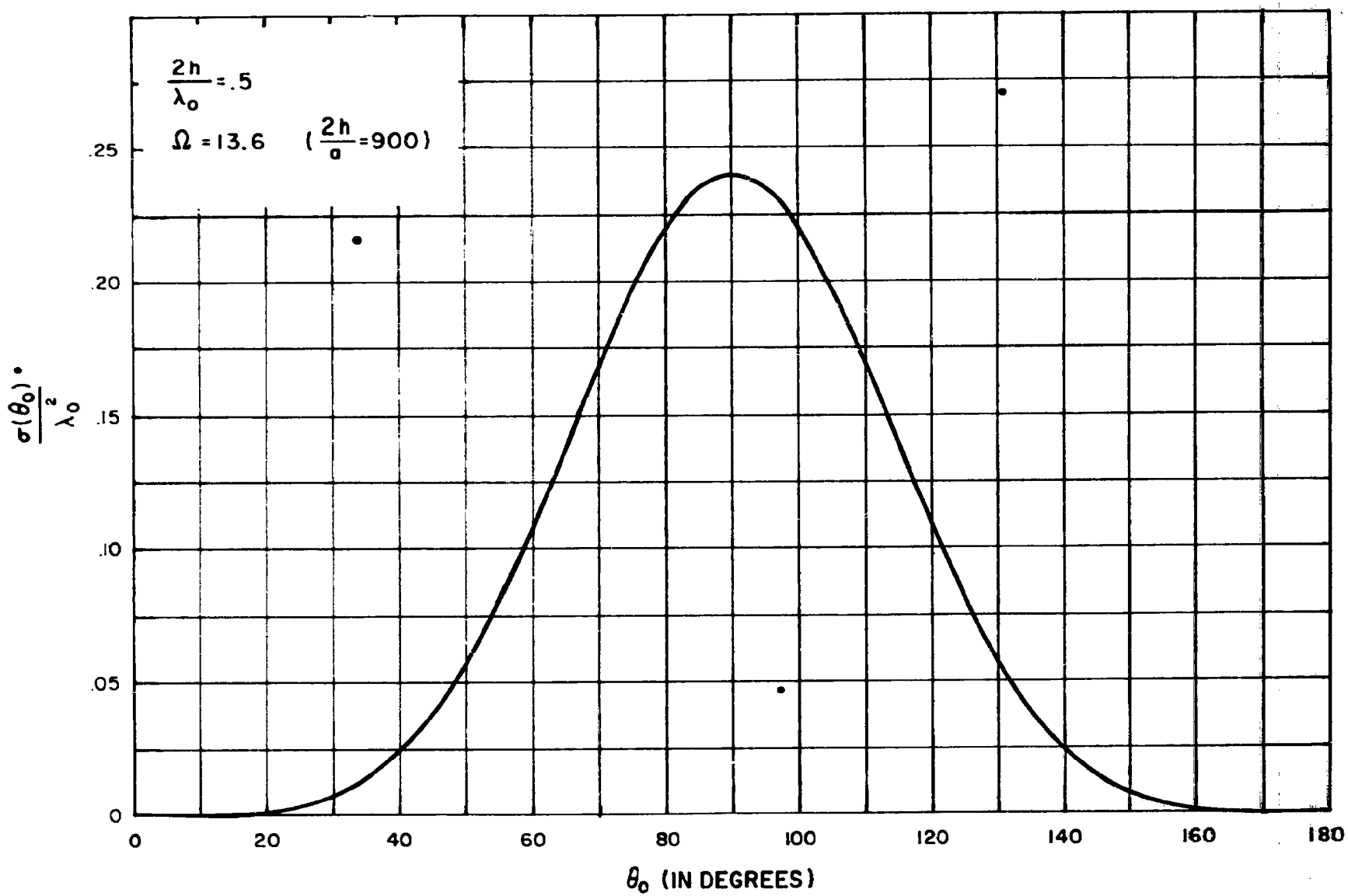

FIGURE 2. ANGULAR DISTRIBUTION OF BACK SCATTER CROSS-SECTION

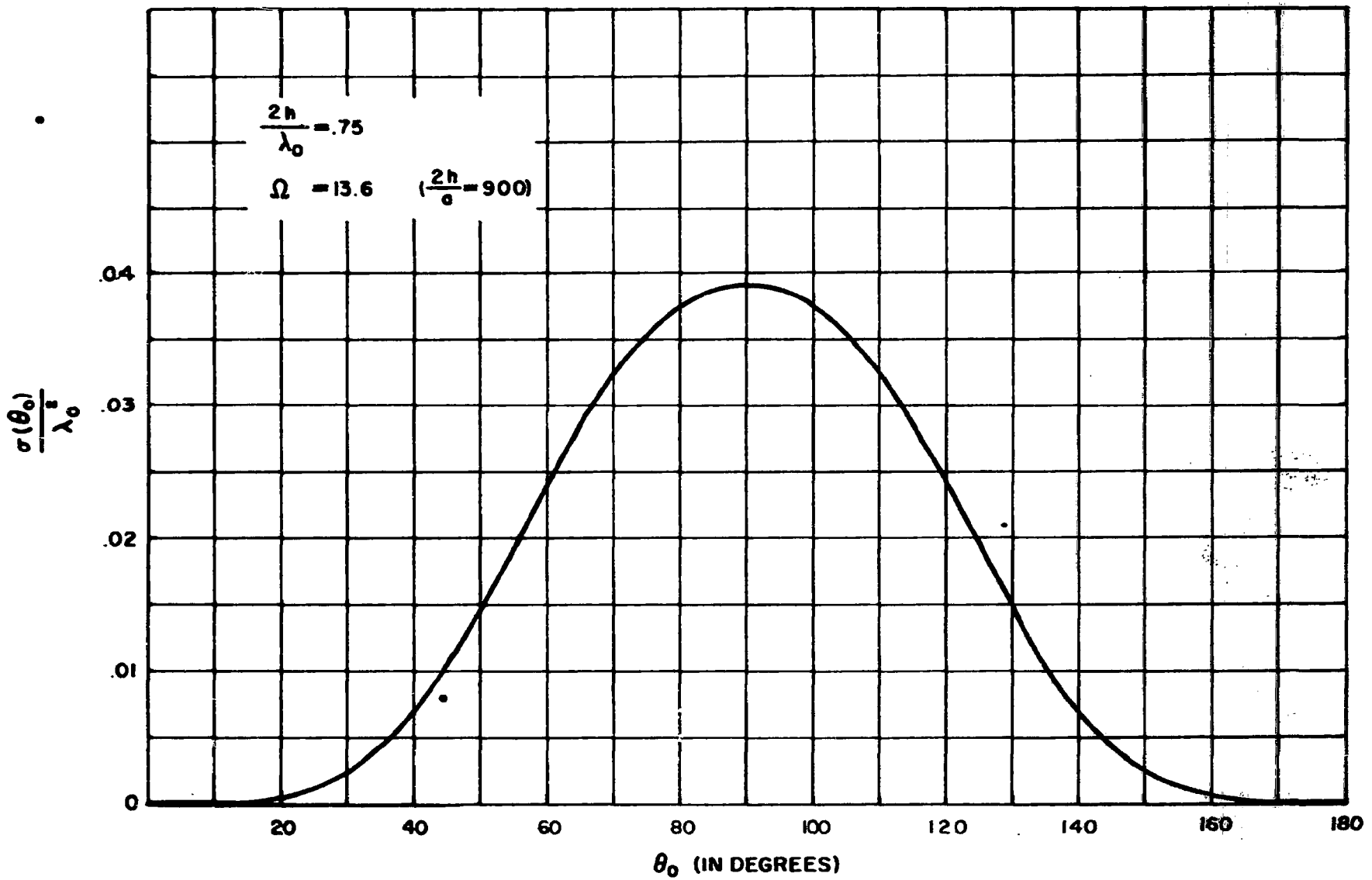

FIGURE 3. ANGULAR DISTRIBUTION OF BACK SCATTER CROSS-SECTION

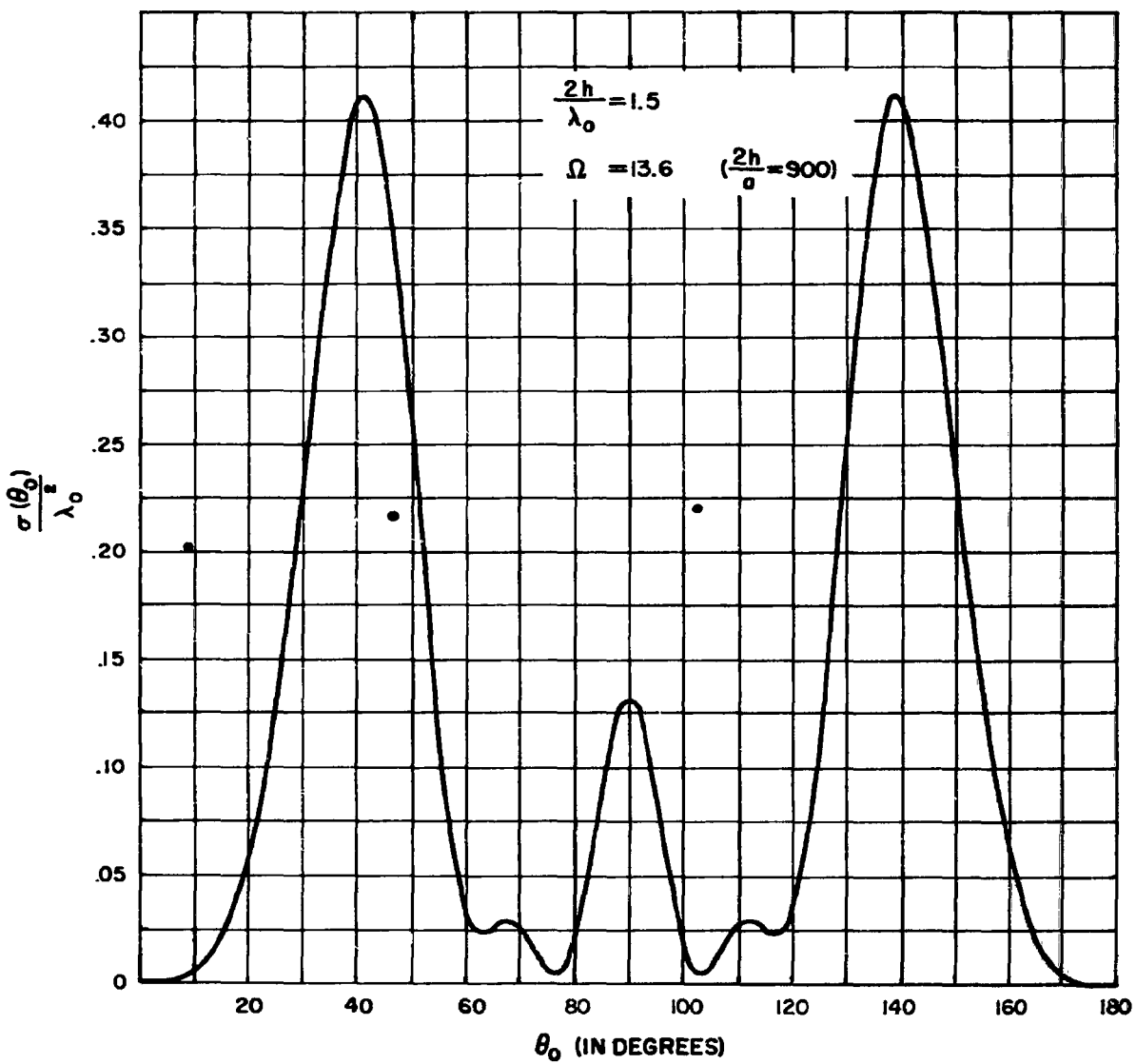

FIGURE 4. ANGULAR DISTRIBUTION OF BACK SCATTER CROSS-SECTION

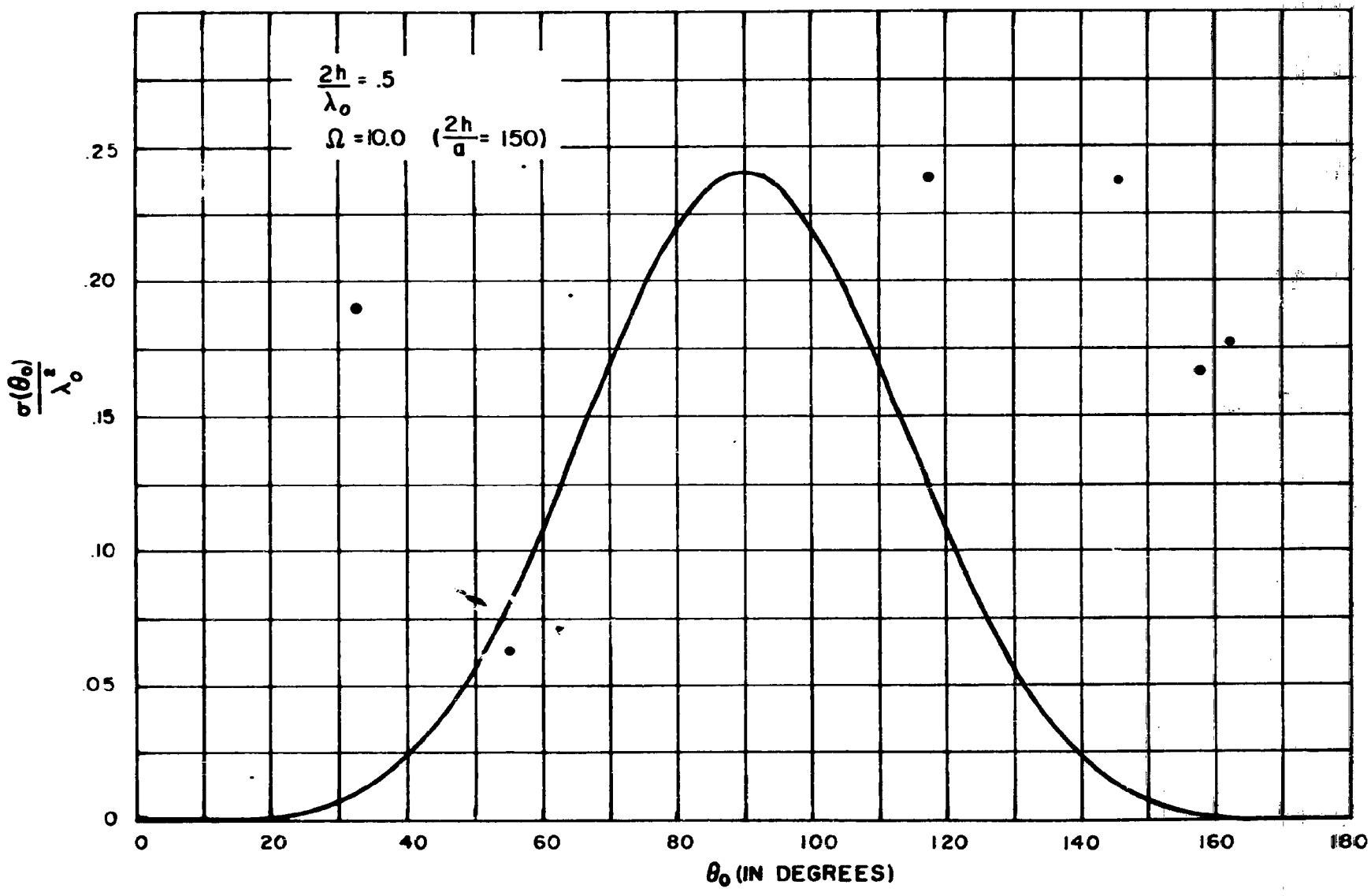

FIGURE 5. ANGULAR DISTRIBUTION OF BACK SCATTER CROSS-SECTION

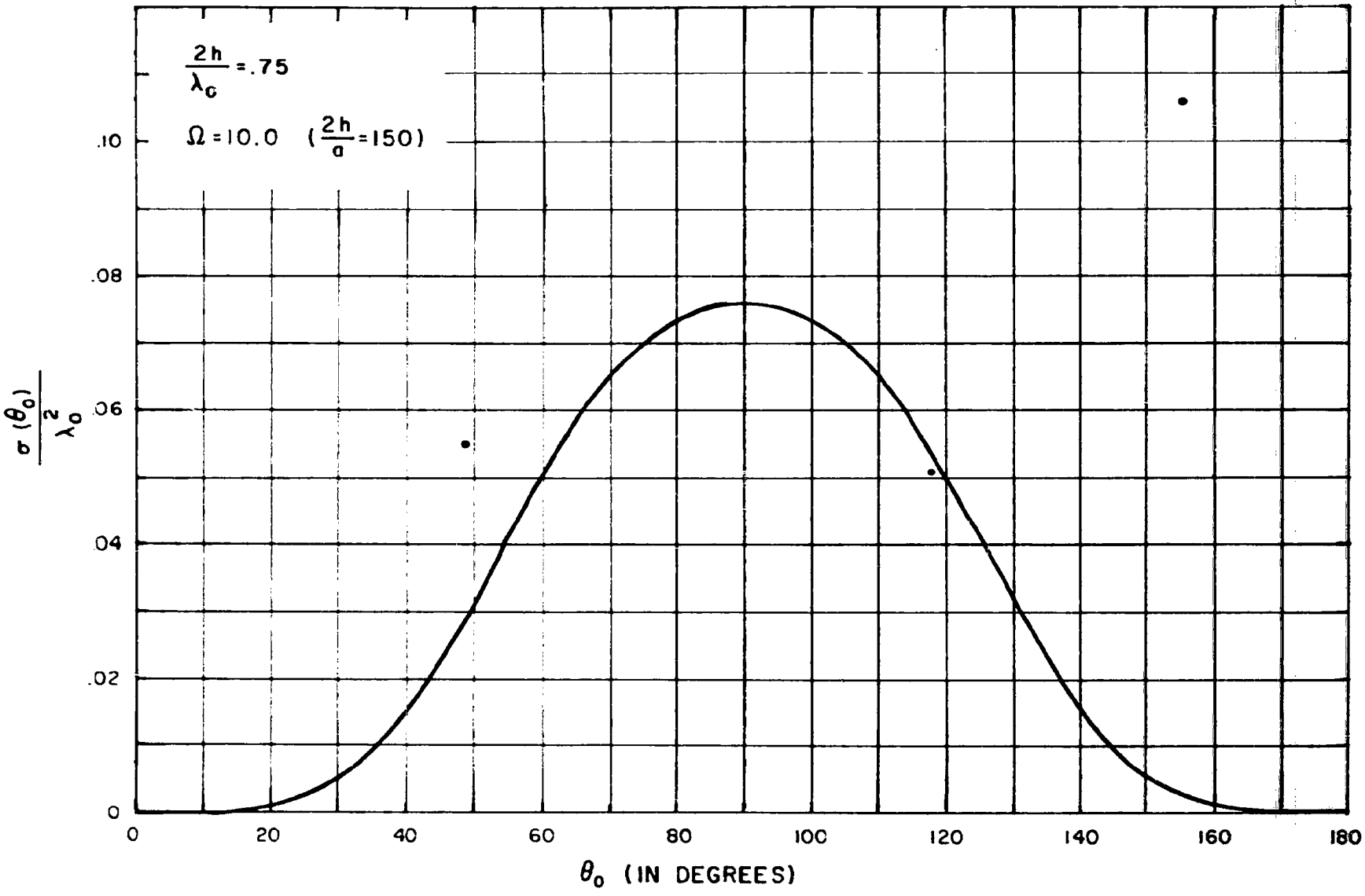

FIGURE 6. ANGULAR DISTRIBUTION OF BACK SCATTER CROSS-SECTION

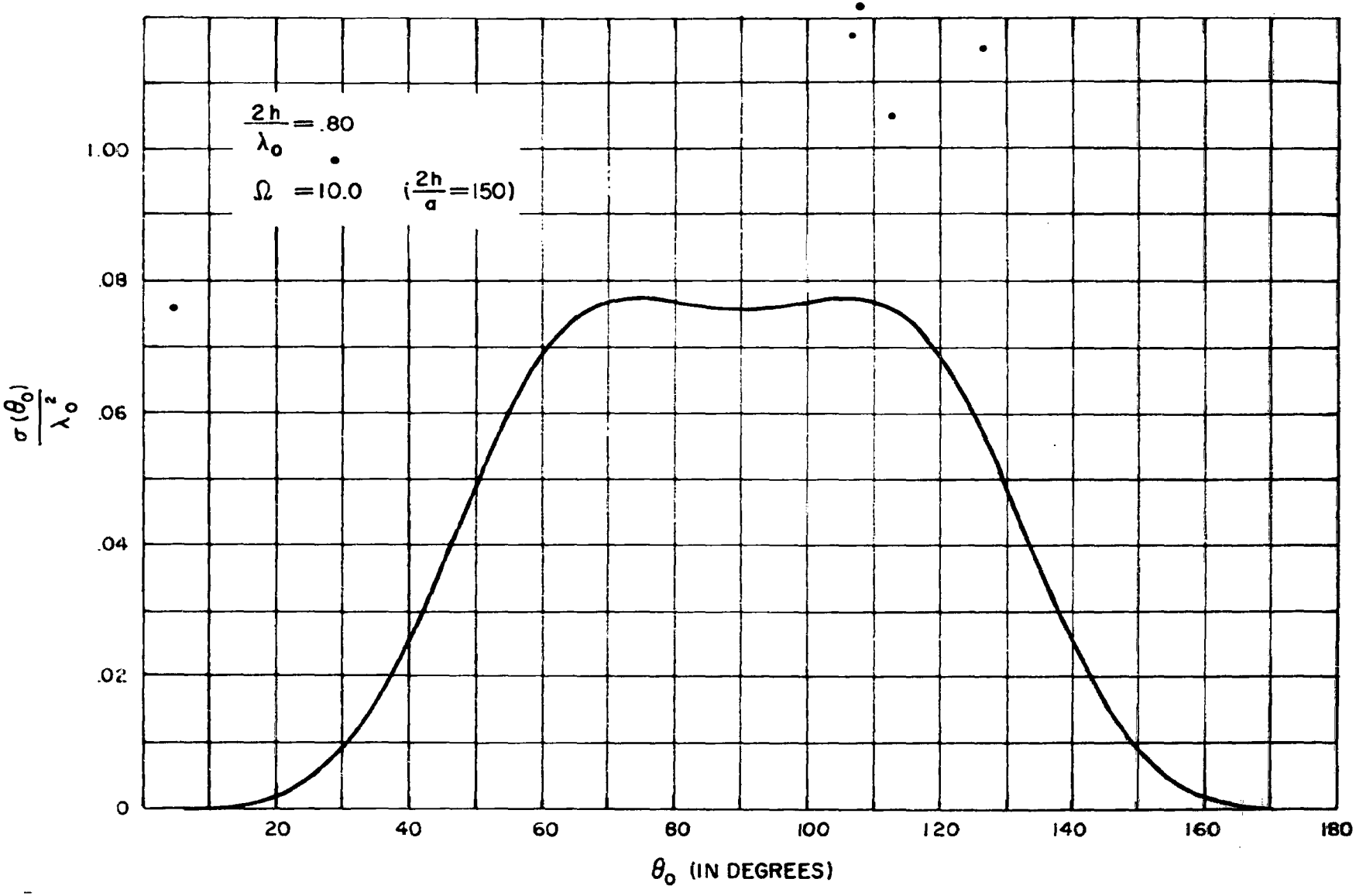

FIGURE 7. ANGULAR DISTRIBUTION OF BACK SCATTER CROSS-SECTION

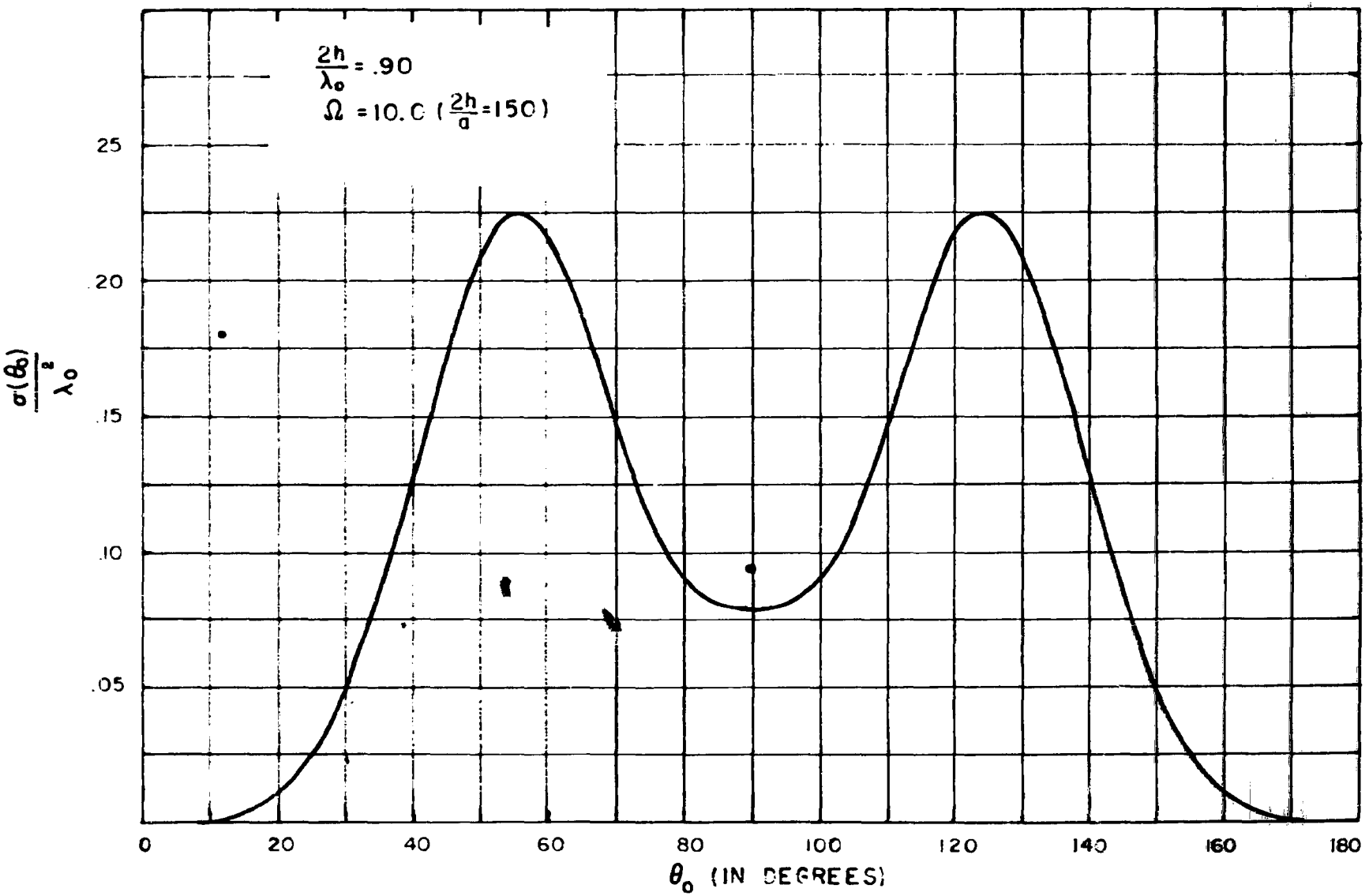

FIGURE 8. ANGULAR DISTRIBUTION OF BACK SCATTER CROSS-SECTION

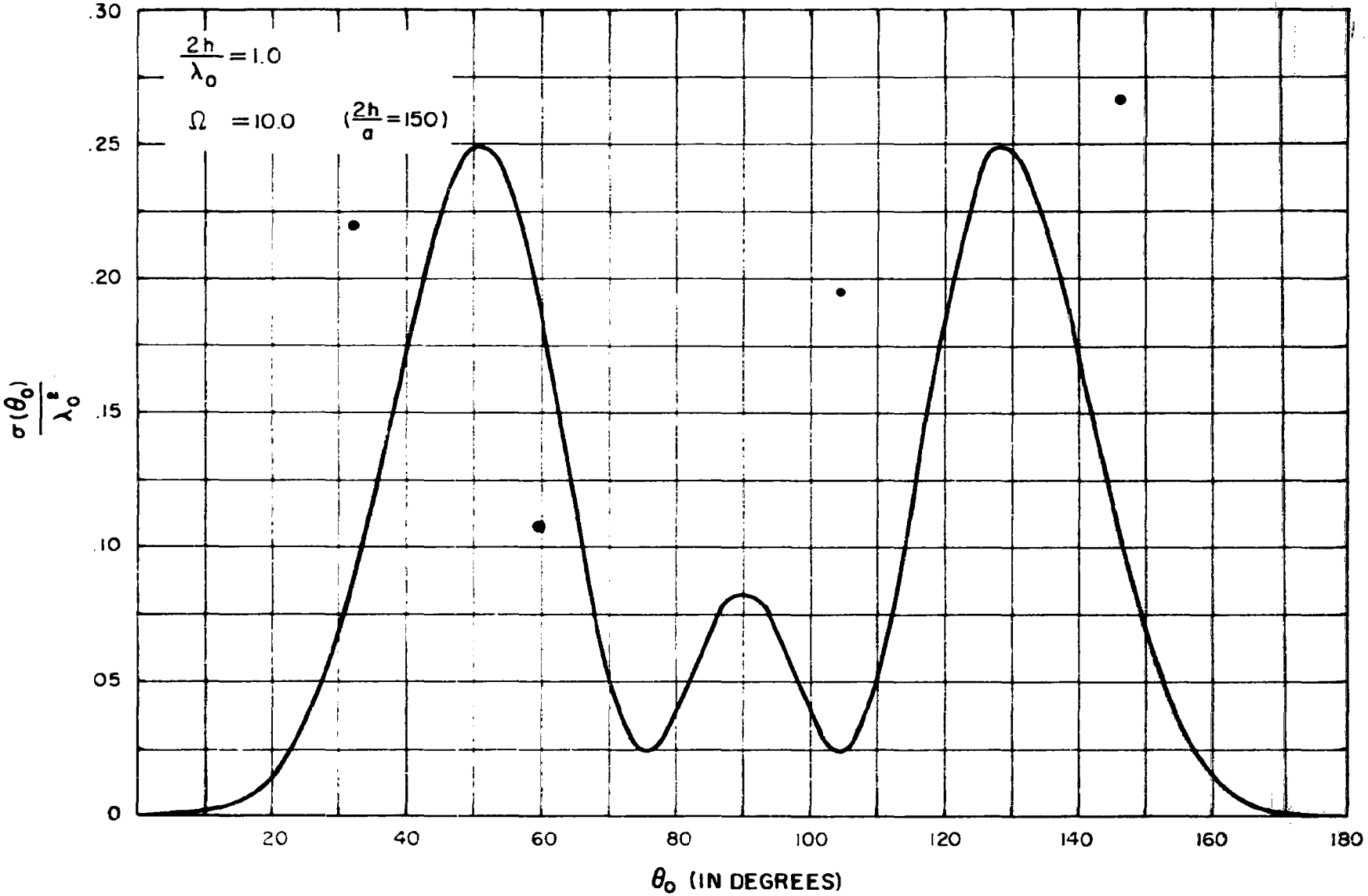

FIGURE 9. ANGULAR DISTRIBUTION OF BACK SCATTER CROSS-SECTION

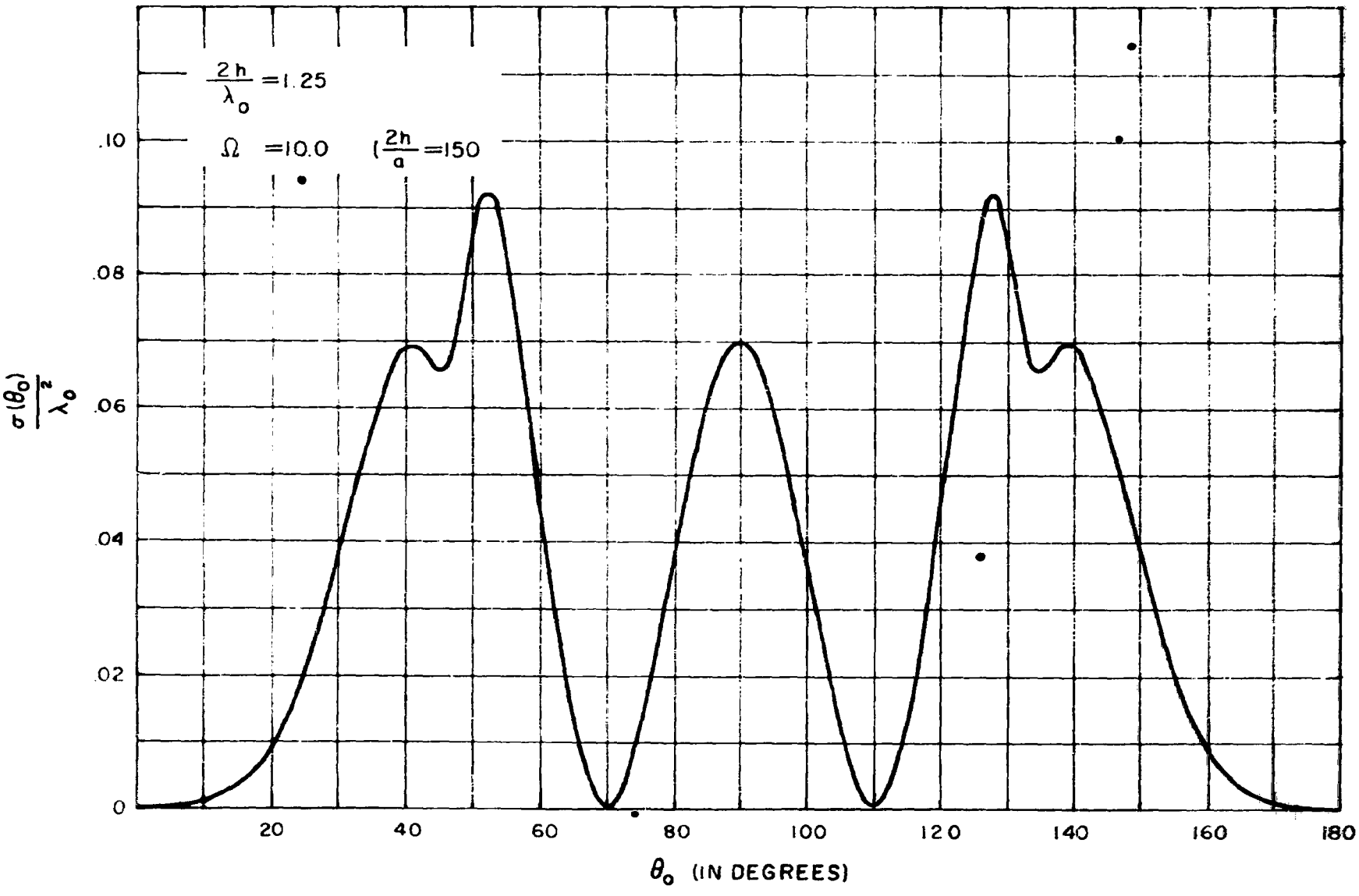

FIGURE 10. ANGULAR DISTRIBUTION OF BACK SCATTER CROSS-SECTION

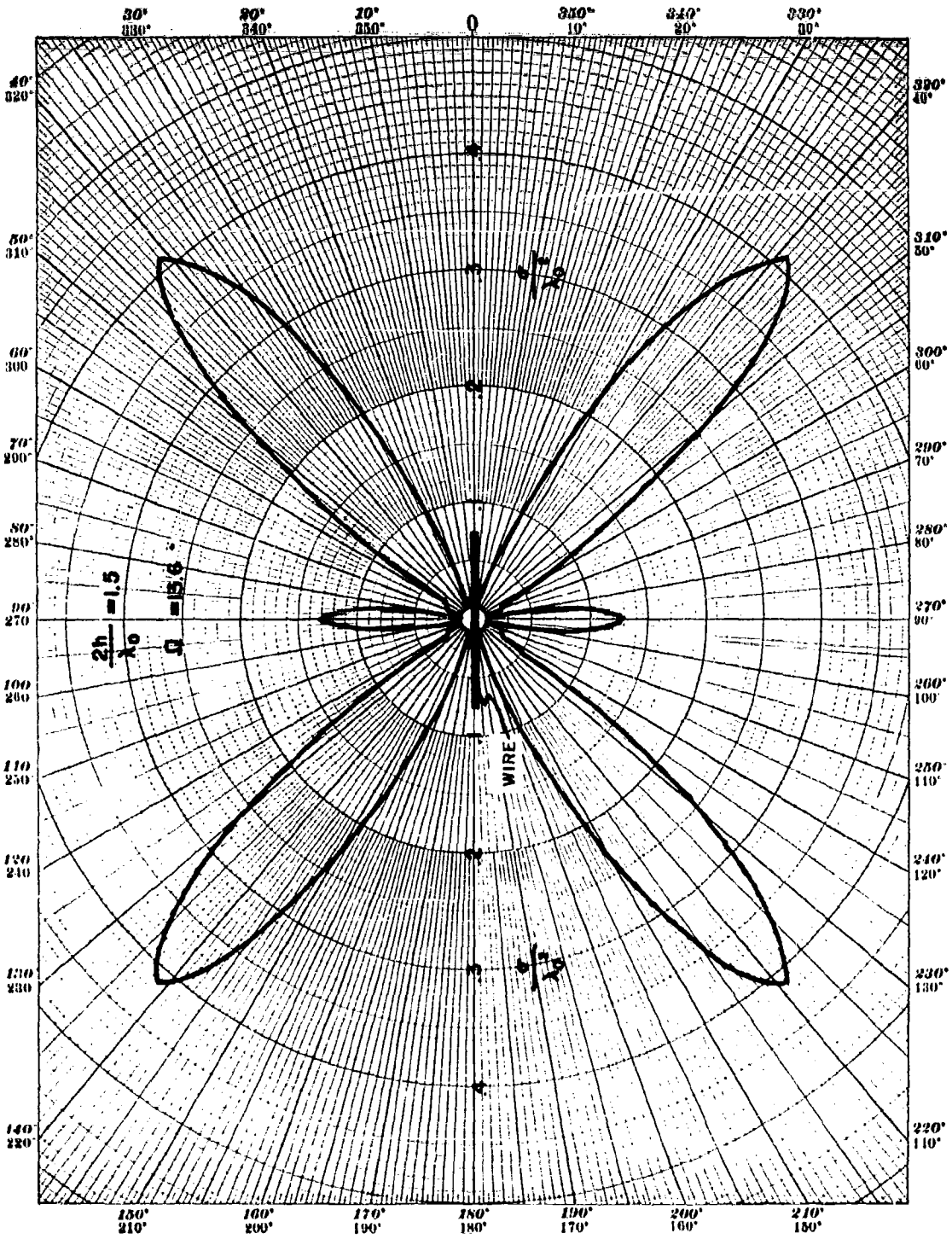

FIGURE II. POLAR PLOT OF BACK SCATTER $\frac{\sigma}{\lambda_0^2}$

$2h/\lambda_o$ increases from 0.75 to 1.25. Apparently the "forced" term and "resonant" term in the current are playing relatively different roles, as mentioned by King[2]. A center-driven antenna $2h/\lambda_o = 1$ has one major lobe, a parasitic scatterer has two lobes as in Figure 9.

The plots given in the above figures are by way of checking the expressions we use with those presented by others plus additional values of cross sections for different values of Ω. The development of the double-lobe is also depicted. These curves show angular response of average cross sections for perfectly conducting parasitic scatterers, $2h/\lambda_o$ lying between 0.5 and 2.0.

We shall now develop bistatic cross sections for the case $\psi = 0$ for perfectly conducting wire scatterers.

III. BISTATIC SCATTERING CROSS SECTIONS

For bistatic scattering, the transmitter (causing the incident field $\underline{E}_{inc}$) and the receiver (detecting the scattered field $\underline{E}_{sc}$) are separated in location. Referring to Figure 12 we shall consider the specialized case where the incident field $\underline{E}_{inc}$ lies in the plane of incidence containing the wire (Z-axis) and the direction of incidence (polarizing angle $\psi = 0$).

The incident field induces a current I(z); the scattered field $\underline{E}_{sc}$ vector lies in the scattering plane containing the direction of the current I(z) (assumed to be the same as the wire or Z-axis) and the direction of propagation of the scattered wave.

I(z) is due to E_i, the amplitude of the incident field and is given by (1). This expression contains the constant A which is given by (6). We need to evaluate I_o in (1). This is done as follows. We start with Tai's expression for the scattering coefficient S, and ultimately given by (7). It is

$$S = \frac{\eta_o \beta_o^2 \sin\theta_o \int_{-h}^{h} I(z) e^{j\beta_o z \cos\theta_o} dz}{4\pi E_i \cos\psi} \qquad (10)$$

$$= \frac{30 \beta_o^2 \sin\theta_o I_o \int (f_c + A f_s) e^{j\beta_o z \cos\theta_o} dz}{E_i \cos\psi}$$

and upon substituting (2)

$$S = 30 \beta_o I_o \frac{g_c + A g_s}{E_i \cos\psi} \qquad (11)$$

Putting in the values of S from (7) and A from (6)

$$I_o = \frac{1}{30\beta_o} \frac{g_c}{\gamma_c} E_i \cos\psi \ .$$

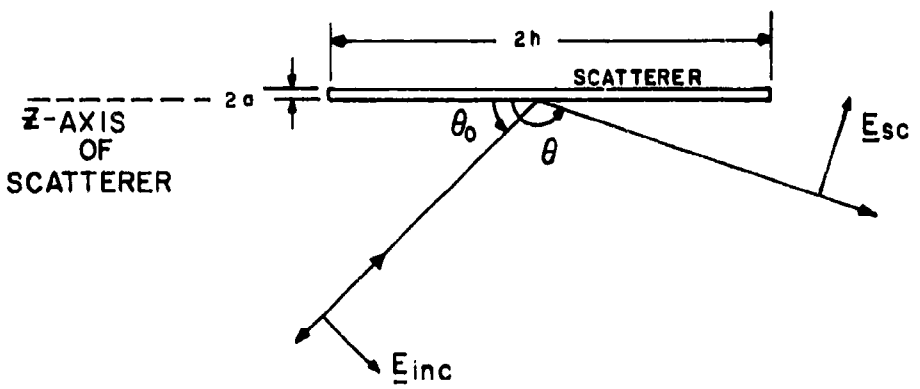

FIGURE 12. GEOMETRY OF BISTATIC SCATTERING ($\underline{E}_{inc}$ LIES IN PLANE OF INCIDENCE)

Now the θ-component of the scattered field E_{sc} in the direction θ, in the far-field at a distance R_o due to I(z), is

$$E_{sc} = -j30\beta_o \sin\theta \frac{e^{-j\beta_o R_o}}{R_o} I_o \int_{-h}^{h} (f_c + Af_s) e^{j\beta_o z\cos\theta} dz \qquad (13)$$

where f_c and f_s are functions of the incident angle θ_o, not the scattering angle θ.

Let us write

$$F = \frac{1}{\beta_o \sin\theta} (G_c + AG_s) = F_c + AF_s \qquad (14)$$

where G_c and G_s are integrals similar to g_c and g_s integrals of Tai but are functions of both θ_o and θ rather than θ_o alone, i.e.

$$G_c = \beta_o \sin\theta \; F_c \qquad G_s = \beta_o \sin\theta \; F_s$$

$$F_c = \int_{-h}^{h} f_c e^{j\beta_o z\cos\theta} dz \qquad F_s = \int_{-h}^{h} f_s e^{j\beta_o z\cos\theta} dz \qquad (15)$$

noting that A is not a function of z.

We now define a bistatic scattering coefficient σ_{BS} for $\psi = 0$ in a fashion similar to that for the radar monostatic case, or

$$\sigma_{BS}(\psi = 0) = 4\pi R_o^2 \left| \frac{E_{sc}}{E_i} \right|_{\psi = 0}$$

$$= \frac{\lambda_o^2}{\pi} \left| S_1 \right|^2 \qquad (16)$$

where the bistatic scattering coefficient $|S_1|$ becomes

$$\left| S_1 \right| = \left| \frac{g_c}{\gamma_c} (G_c + AG_s) \right| = \left| \frac{g_c G_c}{\gamma_c} + \frac{g_s G_s}{\gamma_s} \right| \qquad (17)$$

When $\theta = \theta_o$, i.e. back scattering (radar) $G_c = g_c$, $G_s = g_s$ and $|S_1| = |S|$ in (17).

The G-functions are obtained from evaluating the F-integrals in (6).

We use some abbreviations (which differ a bit from those of Tai). These are

$$\left.\begin{aligned} q &= \beta_o \cos\theta & x &= \beta_o h & \ell &= \beta_o h \cos\theta = x\cos\theta \\ q_o &= \beta_o \cos\theta_o & & & \ell_o &= \beta_o h \cos\theta_o = x\cos\theta_o \end{aligned}\right\} \quad (18)$$

Then

$$\left.\begin{aligned} f_c &= \cos\ell_o \cos\beta_o z - \cos x \cos\ell_o z \\ f_s &= \sin\ell_o \sin\beta_o z - \sin z \sin\ell_o z \end{aligned}\right\} \quad (19)$$

and

$$\left.\begin{aligned} F_c &= \cos\ell_o I_1 - \cos x\, I_2 \\ F_s &= \sin\ell_o I_3 - \sin x\, I_4. \end{aligned}\right\} \quad (20)$$

The values of the various I_n integrals above are

$$\begin{aligned} I_1 &= \int_{-h}^{h} \cos\beta_o z\, e^{jqz}\, dz \\ I_2 &= \int_{-h}^{h} \cos q_o z e^{jqz}\, dz \\ I_3 &= \int_{-h}^{h} \sin\beta_o z e^{jqz}\, dz \\ I_4 &= \int_{-h}^{h} \sin q_o z e^{jqz}\, dz. \end{aligned} \quad (21)$$

Making use of Pierce's Table of Integrals (Nos. 414 and 415) the I-integrals may be evaluated.

$$I_1 = \frac{2}{\beta_o \sin^2\theta} \left(\sin x \cos \ell - \cos\theta \cos x \sin \ell\right) \qquad (22a)$$

$$I_2 = \frac{2}{\beta_o (\cos^2\theta_o - \cos^2\theta)} \left(\cos\theta_o \sin \ell_o \cos \ell - \cos\theta \cos \ell_o \sin \ell\right) \qquad (22b)$$

$$I_3 = j \frac{2}{\beta_o \sin^2\theta} \left(\cos\theta \sin x \cos \ell - \cos x \sin \ell\right) \qquad (22c)$$

$$I_4 = j \frac{2}{\beta_o (\cos^2\theta_o - \cos^2\theta)} \left(\cos\theta \sin \ell_o \cos \ell - \cos\theta_o \cos \ell_o \sin \ell\right) \qquad (22d)$$

The integrals in (22) are thus functions of θ, θ_o and $\beta_o h$, but not the thickness parameter Ω. Evaluating (22) for a set of values of θ, θ_o and x, the results are then substituted in (20) to obtain F_c and F_s and ultimately G_c and G_s in (15). [In a computation routine, the values of (22) are multiplied by $\beta_o \sin\theta$, yielding immediately useful values for the G_c and G_s integrals.]

A set of values of $\sigma_{BS}(\psi = 0)$ were calculated and plotted as a function of the scattering angle θ for various values of θ_o as a parameter. The thickness parameter Ω was chosen as 10 corresponding to $2h/a = 150$. The figures correspond to increasing values of $2h/\lambda_o$ as follows:

Figure 13 $\quad 2h = \frac{\lambda_o}{2} \quad x = \beta_o h = 0.5\pi$

Figure 14 $\quad 2h = \frac{3}{4}\lambda_o \quad x = 0.75\pi$

Figure 15 $\quad 2h = \lambda_o \quad x = 1.0\pi$

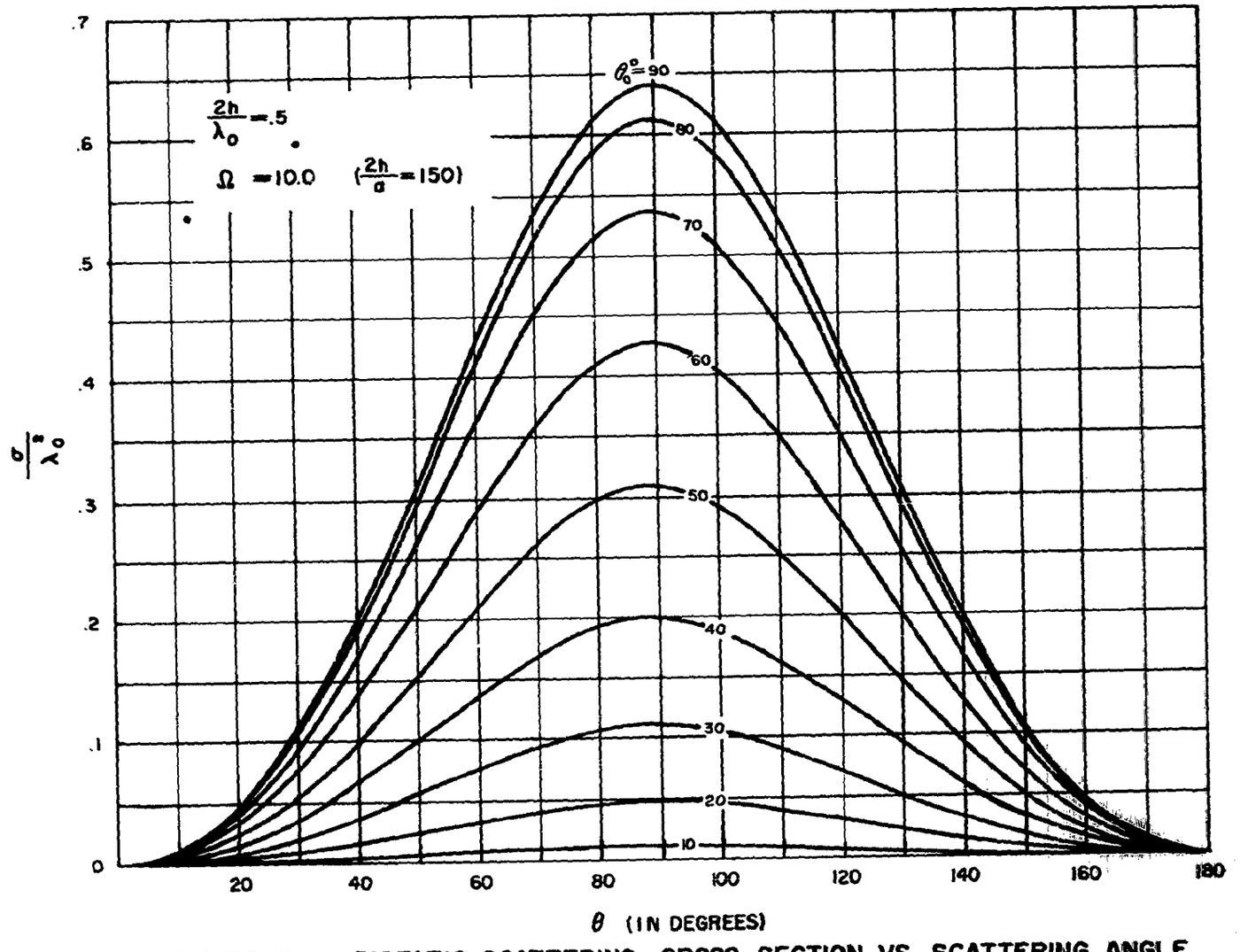

FIGURE 13. BISTATIC SCATTERING CROSS SECTION VS SCATTERING ANGLE

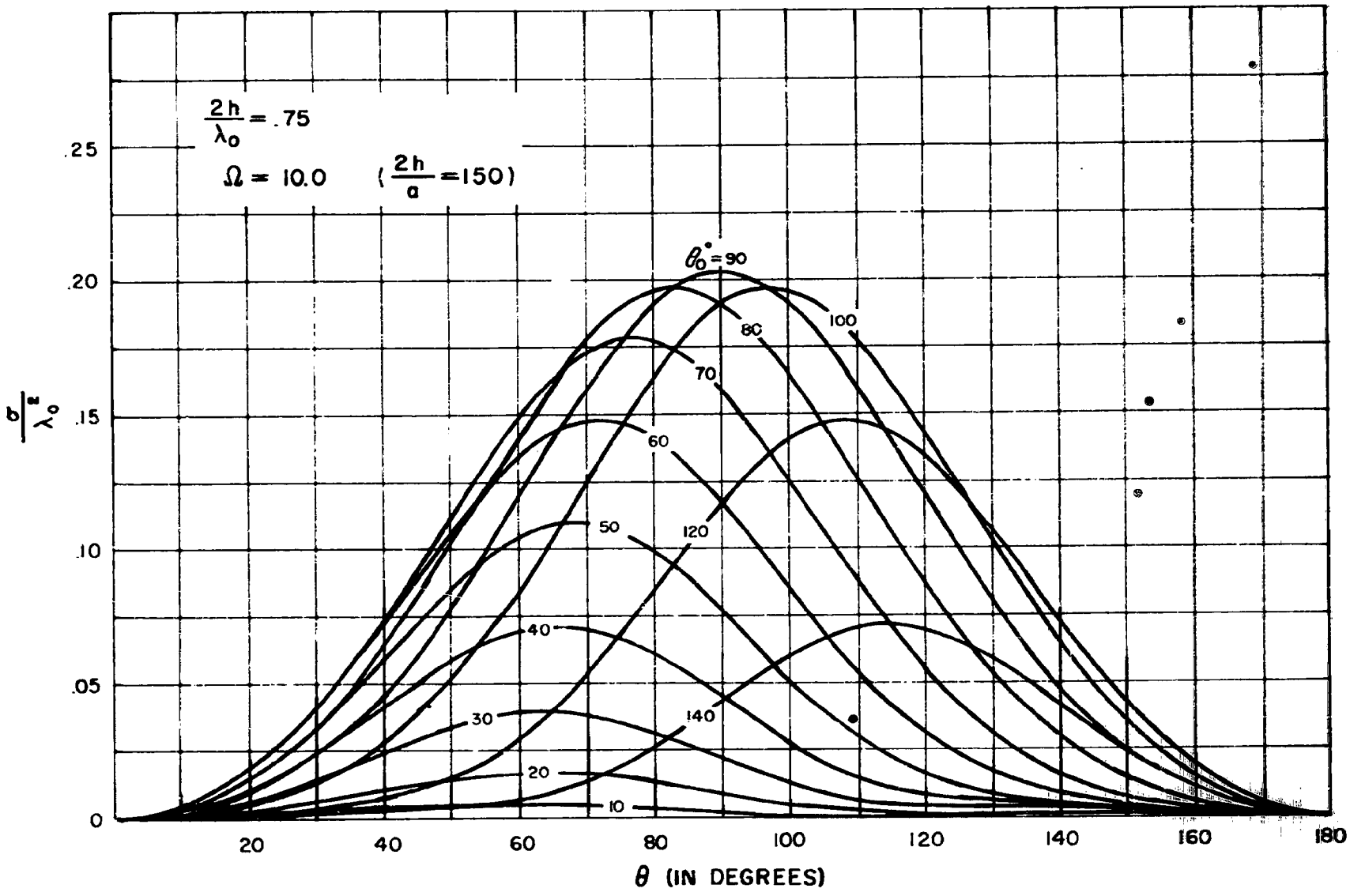

FIGURE 14. BISTATIC SCATTERING CROSS SECTION VS SCATTERING ANGLE

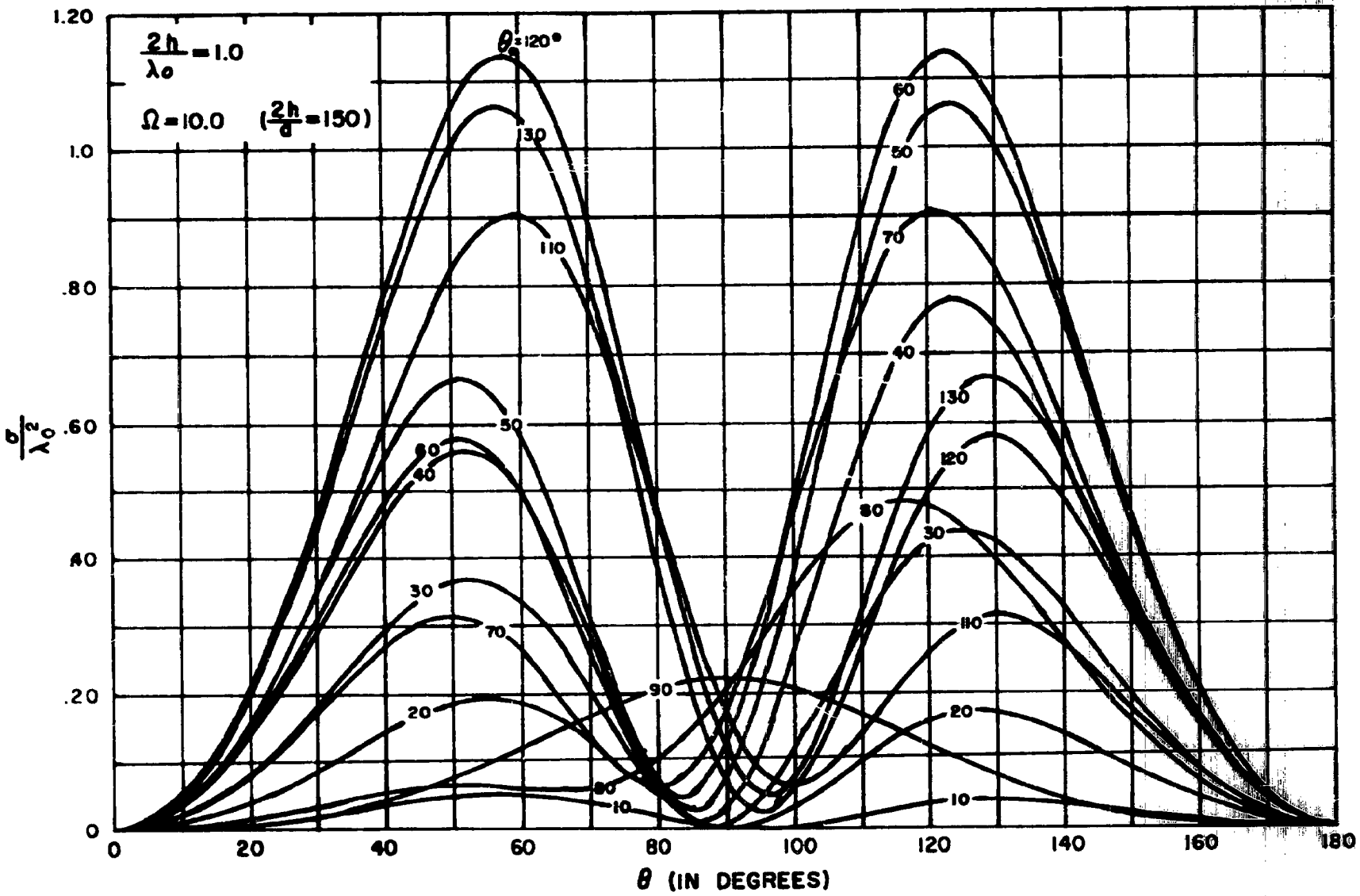

FIGURE 15. BISTATIC SCATTERING CROSS SECTION VS SCATTERING ANGLE

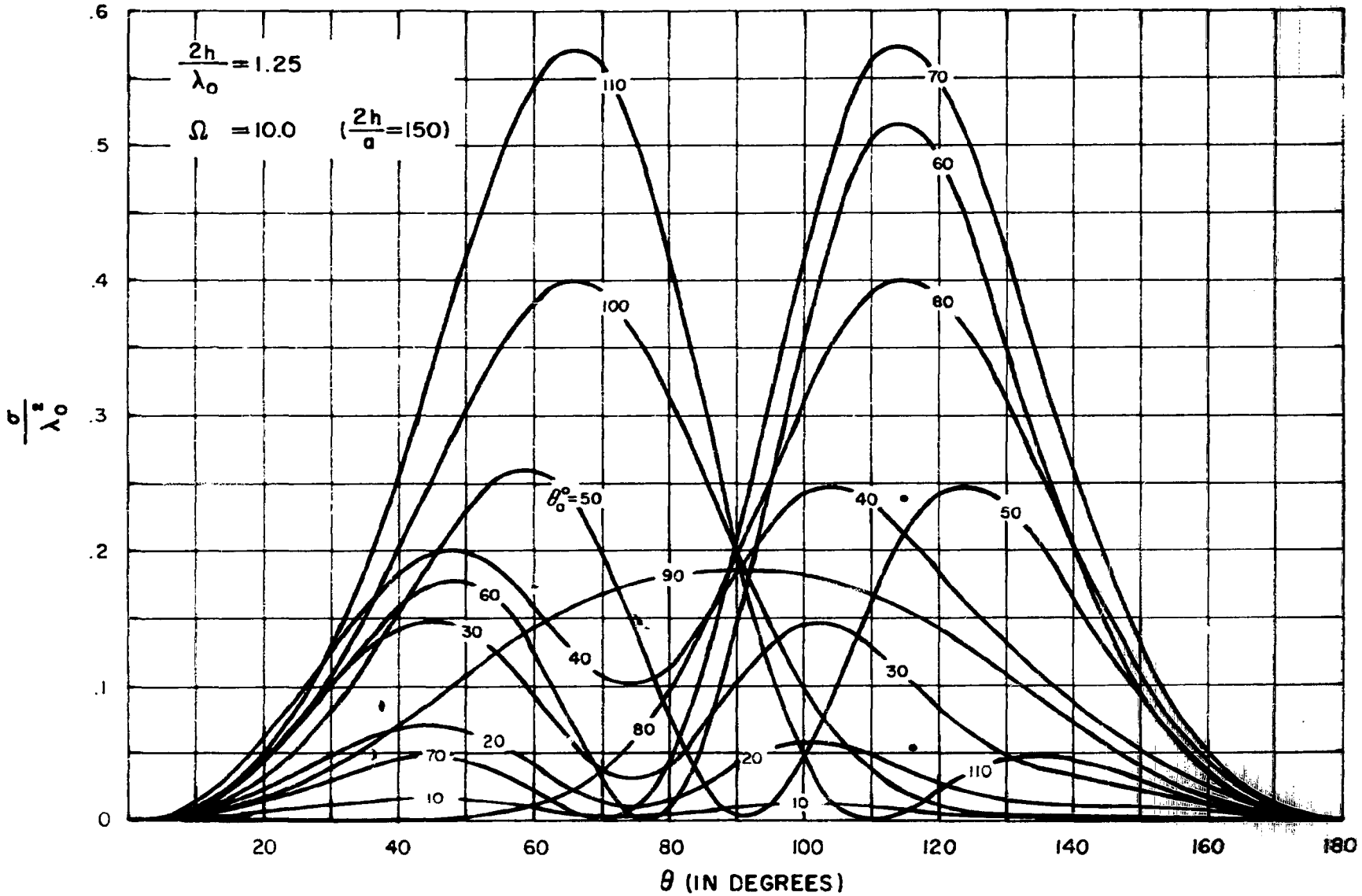

FIGURE 16. BISTATIC SCATTERING CROSS SECTION VS SCATTERING ANGLE

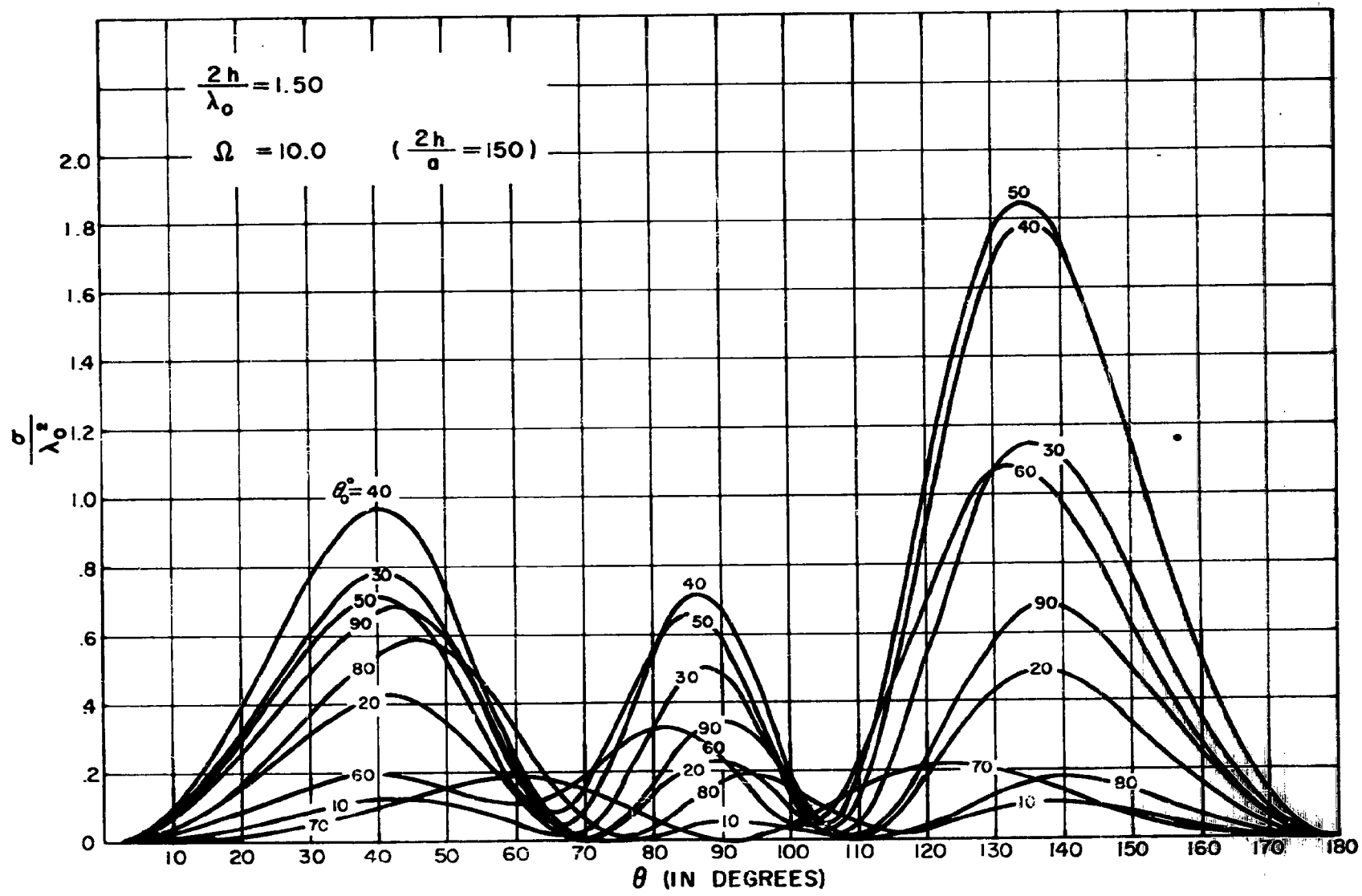

FIGURE 17. BISTATIC SCATTERING CROSS SECTION VS SCATTERING ANGLE

Figure 16 $2h = \frac{5}{4}\lambda_o$ $x = 1.25\pi$

Figure 17 $2h = \frac{3}{2}\lambda_o$ $x = 1.5\pi$

The curves of σ_{BS} are normalized in square wavelengths and apply for $\psi = 0$. (These are not the average values over all values of ψ used in back scatter cross sections of the previous Section.)

Of interest is the asymmetry of σ_{BS}/λ_o^2 ($\psi = 0$) with θ at certain lengths and incident angles. For $2h = \lambda_o/2$, the curves are reasonably symmetrical about $\theta = 90°$ (broadside). However, those for $\frac{2h}{\lambda_o} = 0.75$ begin to show the asymmetry, in that decreasing θ_o below 90° towards smaller values shifts the maximum at values of θ at angles correspondingly less than 90°. A fuller development is shown in Figure 15 for $\frac{2h}{\lambda_o} = 1.0$. Consider here the curve for $\theta_o = 50°$. A lesser maximum occurs in the polar diagram at $\theta = 50°$ than at $\theta = 123°$. When $\theta_o = 130°$ (180° -50°), the larger maximum occurs at 57° (180° - 123°) than at $\theta = 130°$ (180° - 50°). It appears that the asymmetrical curve for $\theta_o = K$ has as a mirror image with varying θ the curve for $\theta_o = 180° - K$.

Thus for certain angles, the cross section is larger in the "forward scatter" region than for "back scatter." Consider Figure 15 again. If $\theta_o = 50°$ and $\theta = 50°$ (back scatter), $\sigma_{BS}/\lambda_o^2 = 0.66$; but at $\theta = 123°$, $\sigma_{BS}/\lambda_o^2 = 1.06$, a ratio of 1.61 or 2 db. This does not always hold true; for example, at $\theta_o = 90°$ there is only one maximum and reception at angles θ greater or less than 90° gives smaller values of σ_{BS}/λ_o^2.

Values of σ_{BS}/λ_o^2 for monostatic (radar) and bistatic scattering are shown below for a few values of θ, $2h/\lambda_o = 1.0$, $\Omega = 10$.

TABLE 1. σ_{BS}/λ_o^2 at $\theta = \theta_o$, $\theta = \theta_1$ (1st Max.) and $\theta = \theta_2$ (2nd Max.) and Ratios to That for Back Scattering ($\theta = \theta_o$)

	$\theta_o = 30°$		$\theta_o = 40°$		$\theta_o = 50°$		$\theta_o = 60°$		$\theta_o = 70°$	
θ ↓	$\theta°$ / $\frac{\sigma}{\lambda_o^2}$	Ratio (db)	$\theta°$ / $\frac{\sigma}{\lambda_o^2}$	Ratio (db)	$\theta°$ / $\frac{\sigma}{\lambda_o^2}$	Ratio (db)	$\theta°$ / $\frac{\sigma}{\lambda_o^2}$	Ratio (db)	$\theta°$ / $\frac{\sigma}{\lambda_o^2}$	Ratio (db)
θ_o	30° / .19	1 (0)	40° / .46	1 (0)	50° / .66	1 (0)	60° / .5	1 (0)	70° / .16	1 (0)
θ_1	52° / .37	1.95 (2.9)	52° / .56	1.08 (.3)	50° / .66	1 (0)	50° / .58	1.16 (.6)	50° / .31	1.94 (2.9)
θ_2	125° / .44	2.37 (3.7)	124° / .78	1.70 (2.3)	123° / 1.06	1.61 (2.0)	123° / 1.14	2.28 (3.6)	121° / .91	5.70 (7.6)

There appears to be an advantage for reception other than at back scatter angles for double hump polar diagrams. The advantage may be at angles closer to the wire than θ_o (viz. $\theta_o = 70°$, with $\theta = \theta_1 = 50°$, there is a 2.9 db advantage over that at $\theta = \theta_o = 70°$); the greater advantage is usually at the second maximum $\theta = \theta_2$ as θ increases from 0 to 180°.

In the case of $2h/\lambda_o = 0.75$ (Figure 14), exhibiting a single lobe, the advantage is only slight for scattering on the maxima vs back scattering until very small values of θ_o are employed.

IV. THE CURRENT DISTRIBUTION I(z)

A clue to the behavior of multi-lobed scattering polar diagrams, particularly for $2h > \lambda_o/2$, can be found in an examination of the current distributions.

The current distribution, assumed axial, is given by (1)

$$I(z) = I_o \left[f_c(z) + A f_s(z) \right] \tag{1}$$

where $f_c(z)$ and $f_s(z)$ are given by (2).

The constant A is given by equation (6) as

$$A = \frac{g_s \ \gamma_c}{g_c \ \gamma_s} \tag{6}$$

with the integrals g_s, g_c, γ_c, and γ_s defined by 8(a), (b), (c) and (d) and evaluated in the Appendix. The constant I_o is given by (12) as

$$I_o = \frac{1}{30 \ \beta_o} \frac{g_c}{\gamma_c} \ E_i \cos \psi \tag{12}$$

where $\beta_o = 2\pi / \lambda_o$, E_i is the amplitude of the incident wave and ψ the polarization angle (Figure 1).

Substituting (12) and (6) in (1), we may obtain a normalized current distribution which we call I, viz.

$$I = \frac{I(z) \ 30 \ \beta_o}{E_i \cos \psi} = \frac{g_c}{\gamma_c} \left[f_c(z) + A f_s(z) \right] \tag{23}$$

$$= \frac{g_c}{\gamma_c} f_c(z) + \frac{g_s}{\gamma_s} f_s(z)$$

which we may write in polar form

$$I = \left| I \right| e^{j \theta_I} \tag{24}$$

Computations of $|I|$ and θ_I were made for $\Omega = 10$ and for $2h = \frac{\lambda_o}{2}$ ($x = \pi/2$) and $2h = \lambda_o (x = \pi)$, to illustrate the behavior of I.

The variations of $|I|$ and θ_I vs z/h for $2h = \lambda_o/2$ ($x = \pi/2$) are shown in Figures 18 and 19 respectively. The variations of $|I|$ for $2h = \lambda_o (x = \pi)$ vs z/h are shown in Figures 20(a) and (b) and the phase angle θ_I in Figures 21(a) and (b).

Regarding the case $2h = \lambda_o/2$, a single maximum occurs in $|I|$, Figure 18, for all values of θ_o. The phase angle variations, all in the fourth quadrant, indicate a single peak in the scattered field with asymmetry due to θ_I.

For $2h = \lambda_o (x = \pi)$, there are principally two maxima in $|I|$, and these are asymmetrical. The phase angles shift from the third quadrant $-1 \leq z/h < o$ to the first quadrant for $z/h > 0$. When $\theta_o = 90°$ (broadside incidence), the single broad peak with a constant θ_I indicates a small single peak in the scattered field.

The current distribution (23) can be considered due to a "forced" component and a "resonant" component, as suggested by King[2] (Chapter IV). The "forced" terms contain trigonometric terms in $\beta_o \cos \theta_o z$, whence they depend upon the phase of the electric field along the wire. The other "resonant" terms depend upon $\beta_o z$ only.

We write

$$I = I_F + I_R$$

where

$$I_F = -\left[\frac{g_c}{\gamma_c} \cos x \cos\left(x \cos\theta_o \frac{z}{h}\right) + \frac{\beta_s}{\gamma_s} \sin x \sin\left(x \cos\theta_o \frac{z}{h}\right)\right] \quad (25)$$

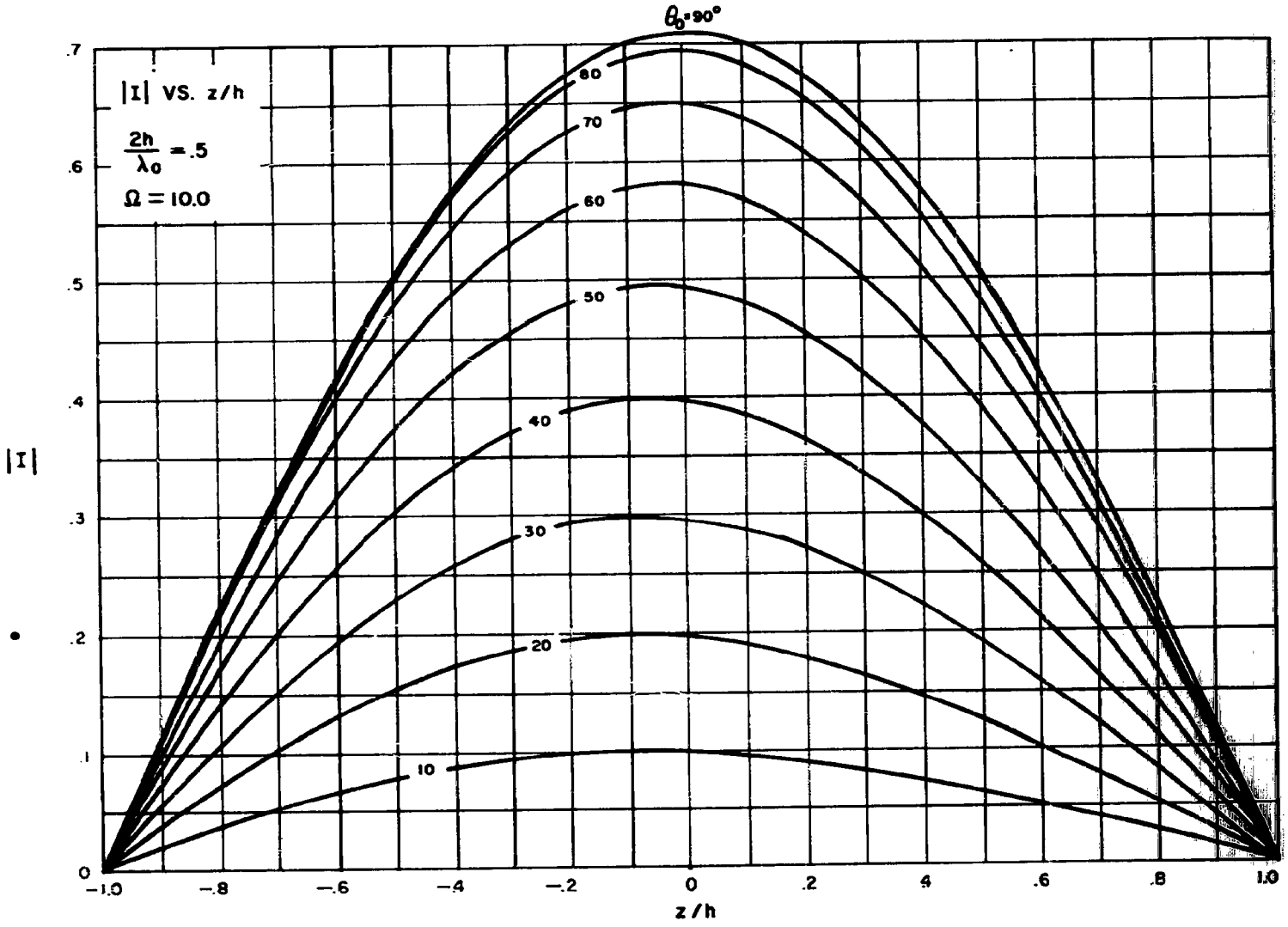

FIGURE 18. DISTRIBUTION OF CURRENT $I=|I|e^{j\theta_I}$

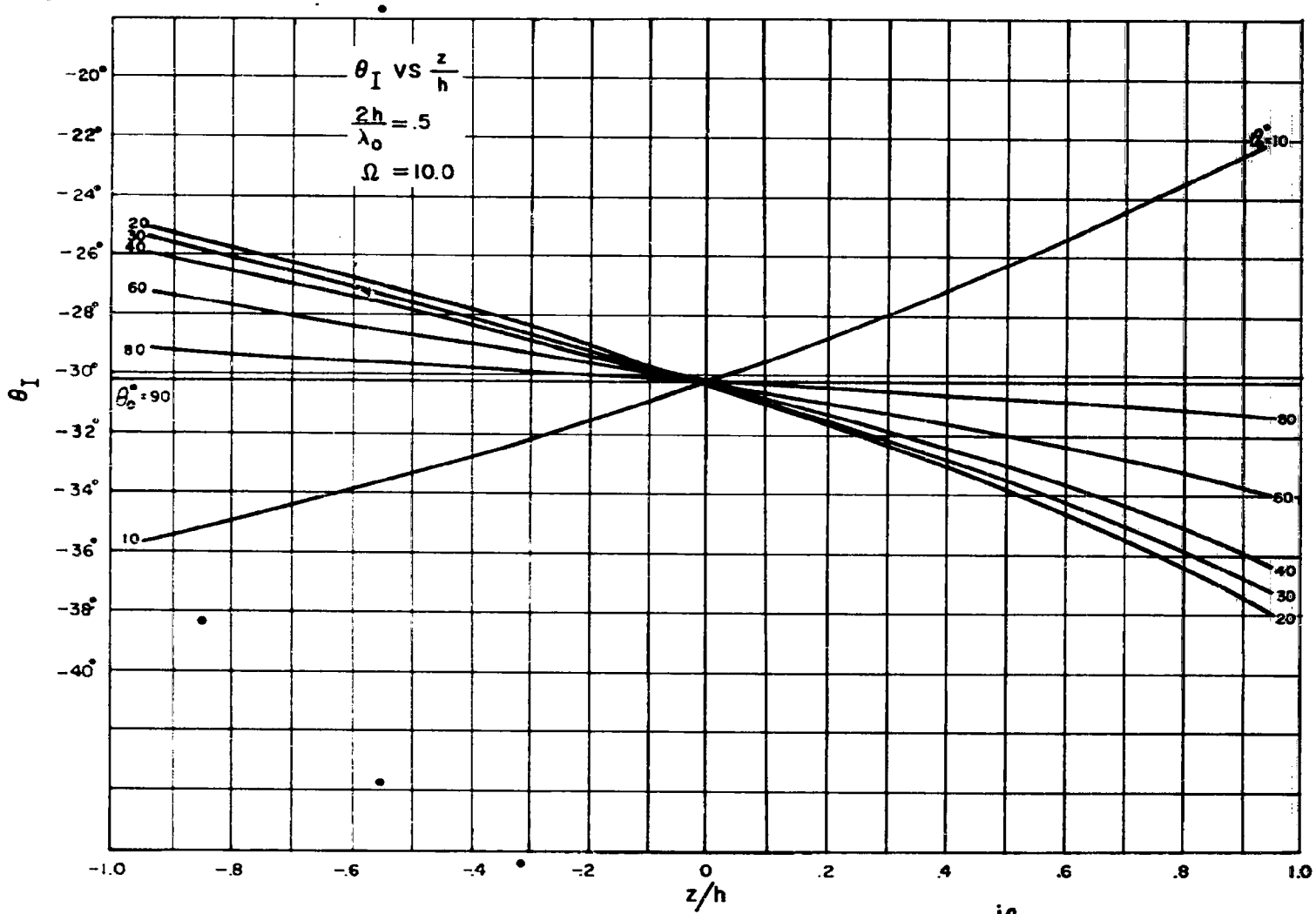

FIGURE 19. DISTRIBUTION OF CURRENT $I = |I| e^{j\theta_I}$

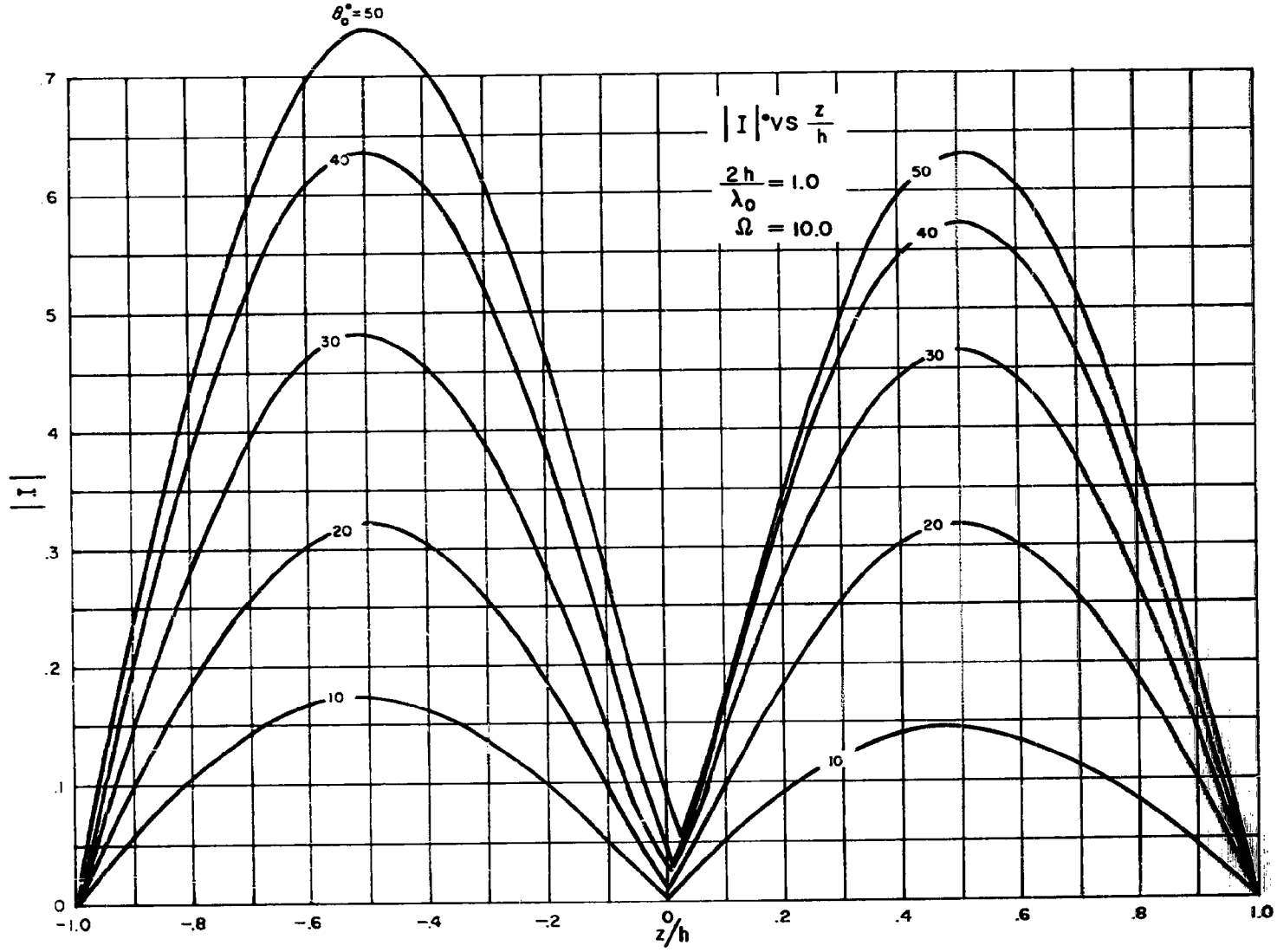

FIGURE 20a. DISTRIBUTION OF CURRENT $I = |I| e^{j\theta I}$

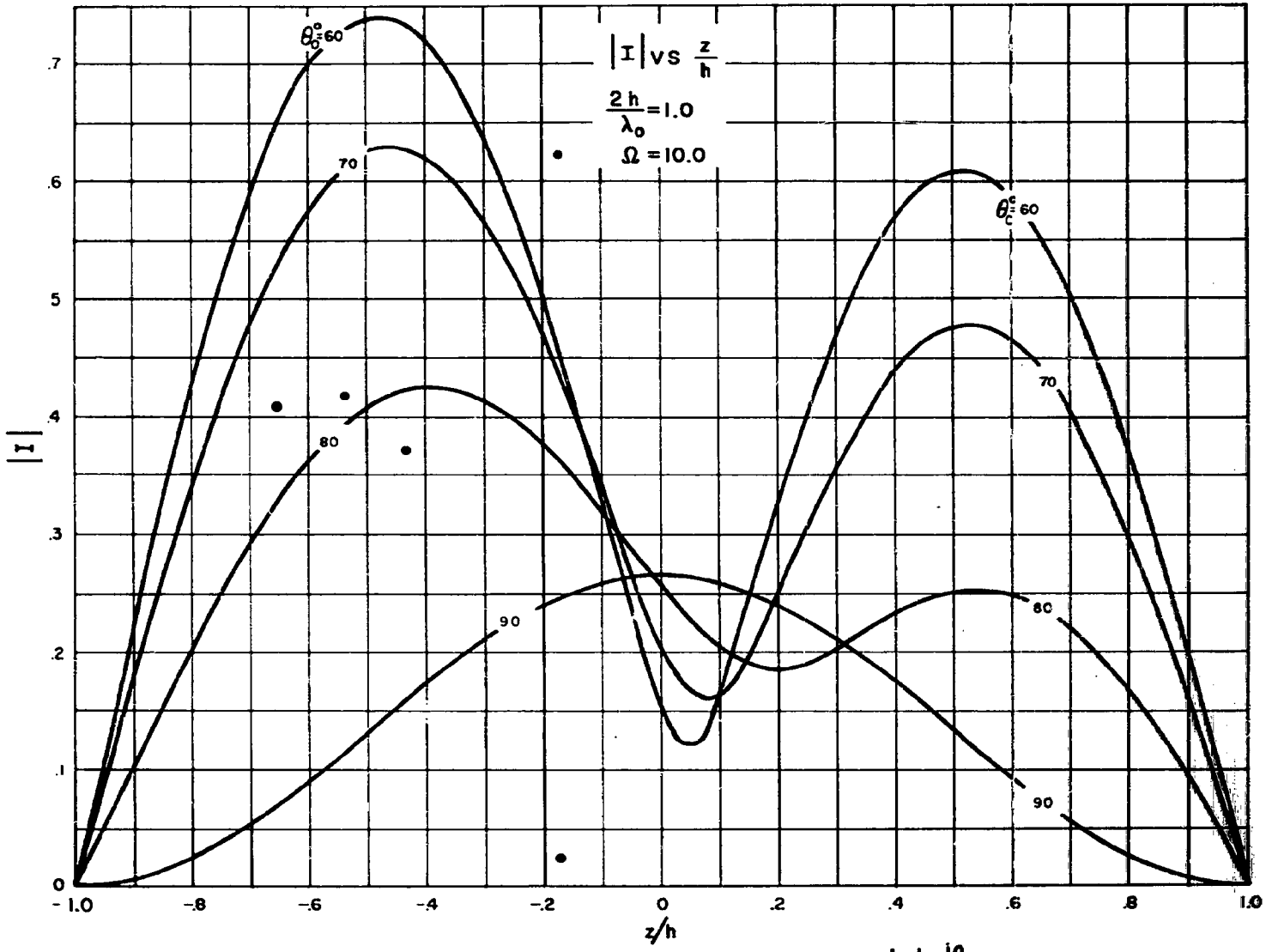

FIGURE 20b. DISTRIBUTION OF CURRENT $I=|I|e^{j\theta_I}$

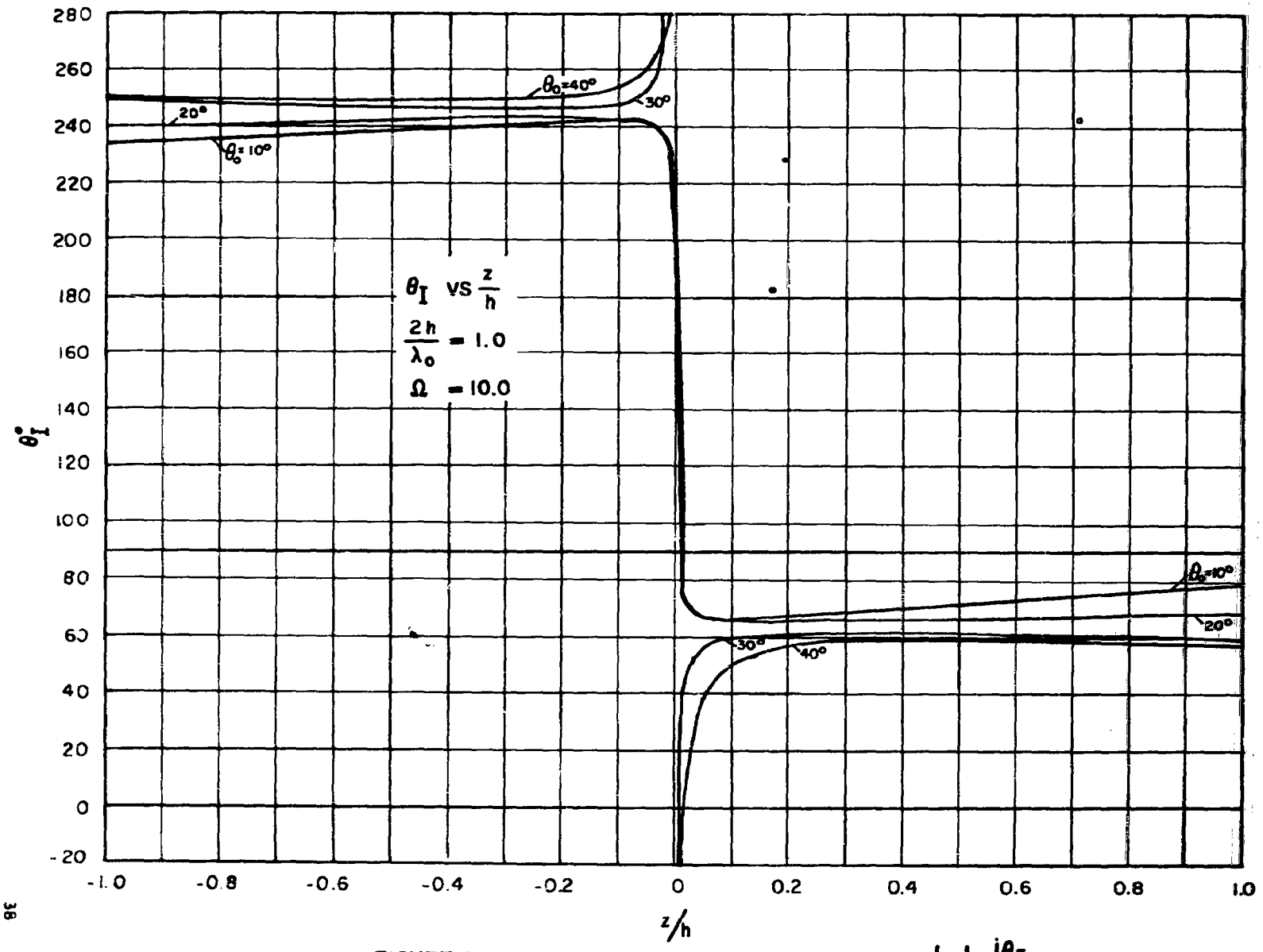

FIGURE 21a. DISTRIBUTION OF CURRENT $I = |I| e^{j\theta_I}$

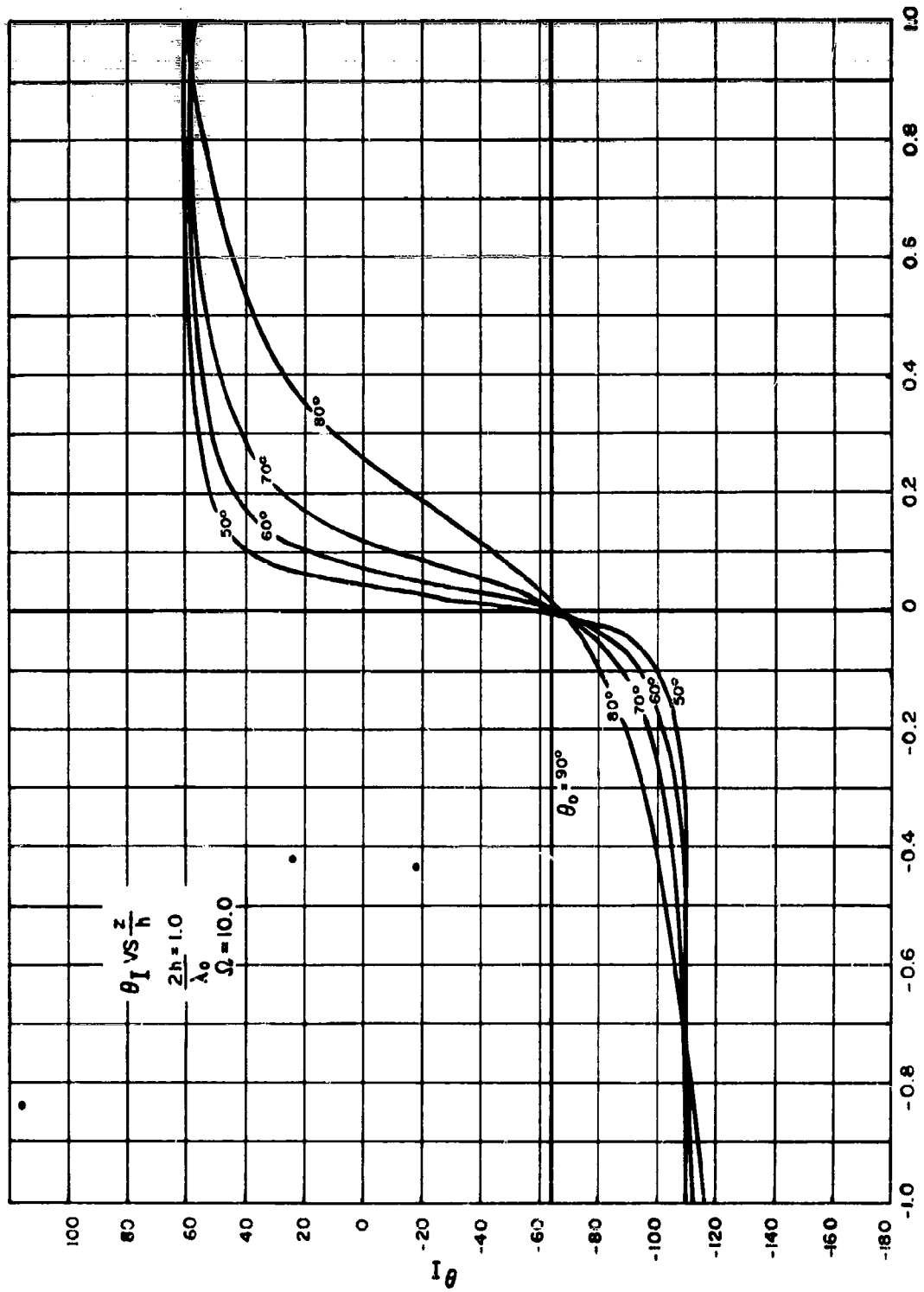

FIGURE 21b. DISTRIBUTION OF CURRENT $I = |I| e^{j\theta_I}$

$$I_R = + \left[\frac{g_c}{\gamma_c} \cos (x \cos \theta_o) \cos (x \frac{z}{h}) + \frac{g_s}{\gamma_s} \sin (x \cos \theta_o) \sin (x \frac{z}{h}) \right] \quad (26)$$

where

$$x \frac{z}{h} = \beta_o h \frac{z}{h} = \beta_o z$$

$$x \cos \theta_o \frac{z}{h} = \beta_o z \cos \theta_o.$$

We find that at broadside incidence, $\theta_o = 90°$, the contribution of I_R to the total current is 100% ($I_F = 0$) when $2h = \lambda_o/2$ ($x = \pi/2$) but is 50% when $2h = \lambda_o$ ($x = \pi$) and $z/h = 0$.

Plots of $I_F = \left| I_F \right| e^{j\theta_F}$ and $I_R = \left| I_R \right| e^{j\theta_R}$ are shown, for $2h = \lambda_o/2$, in Figures 22 and 23 for I_F and Figures 24 and 25 for I_R. These curves illustrate the relative effects of I_F and I_R by comparison with the total current I (Figures 18 and 19).

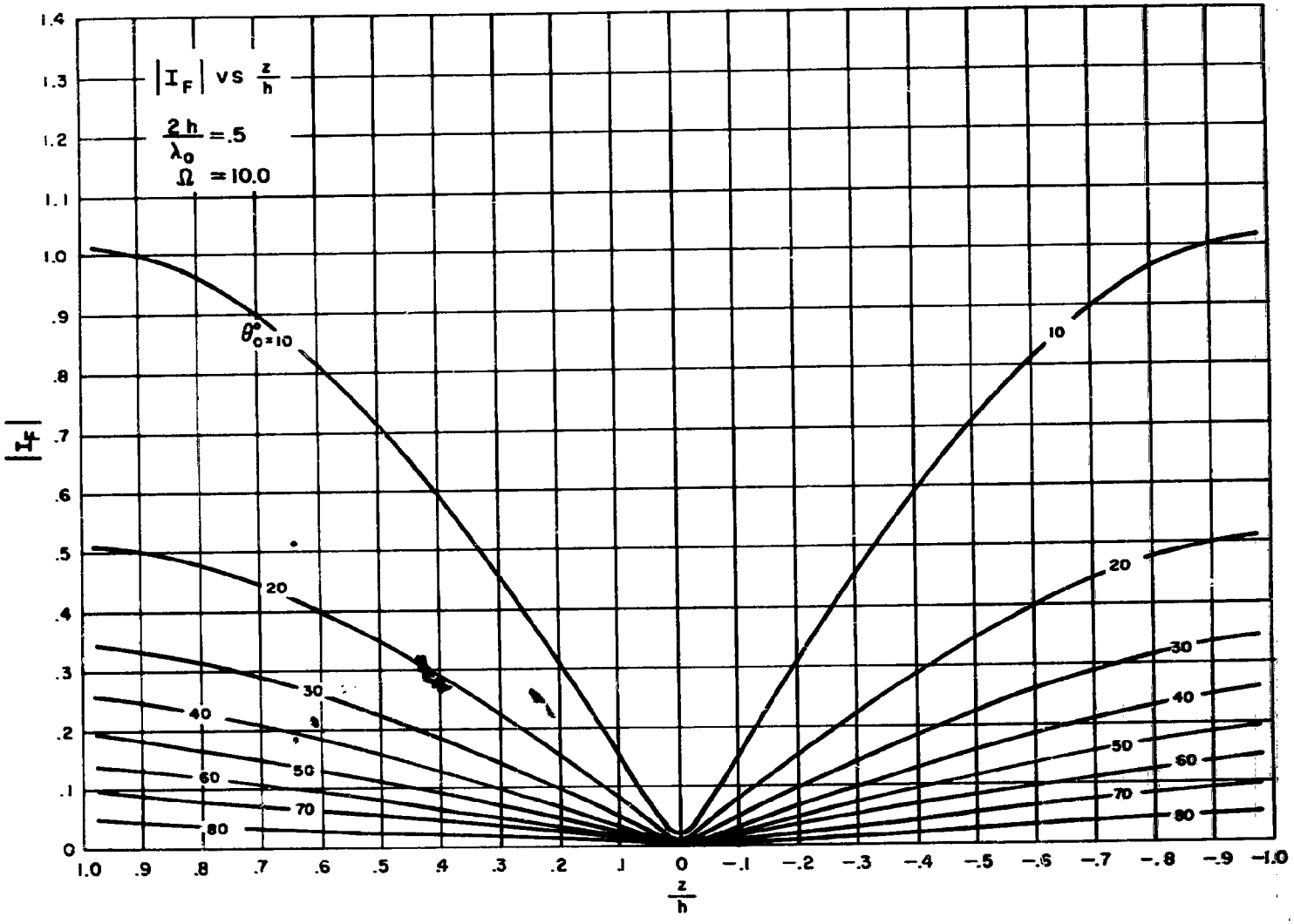

FIGURE 22. DISTRIBUTION OF "FORCED COMPONENT OF CURRENT"

$$I_F = |I_F| e^{j\theta_F}$$

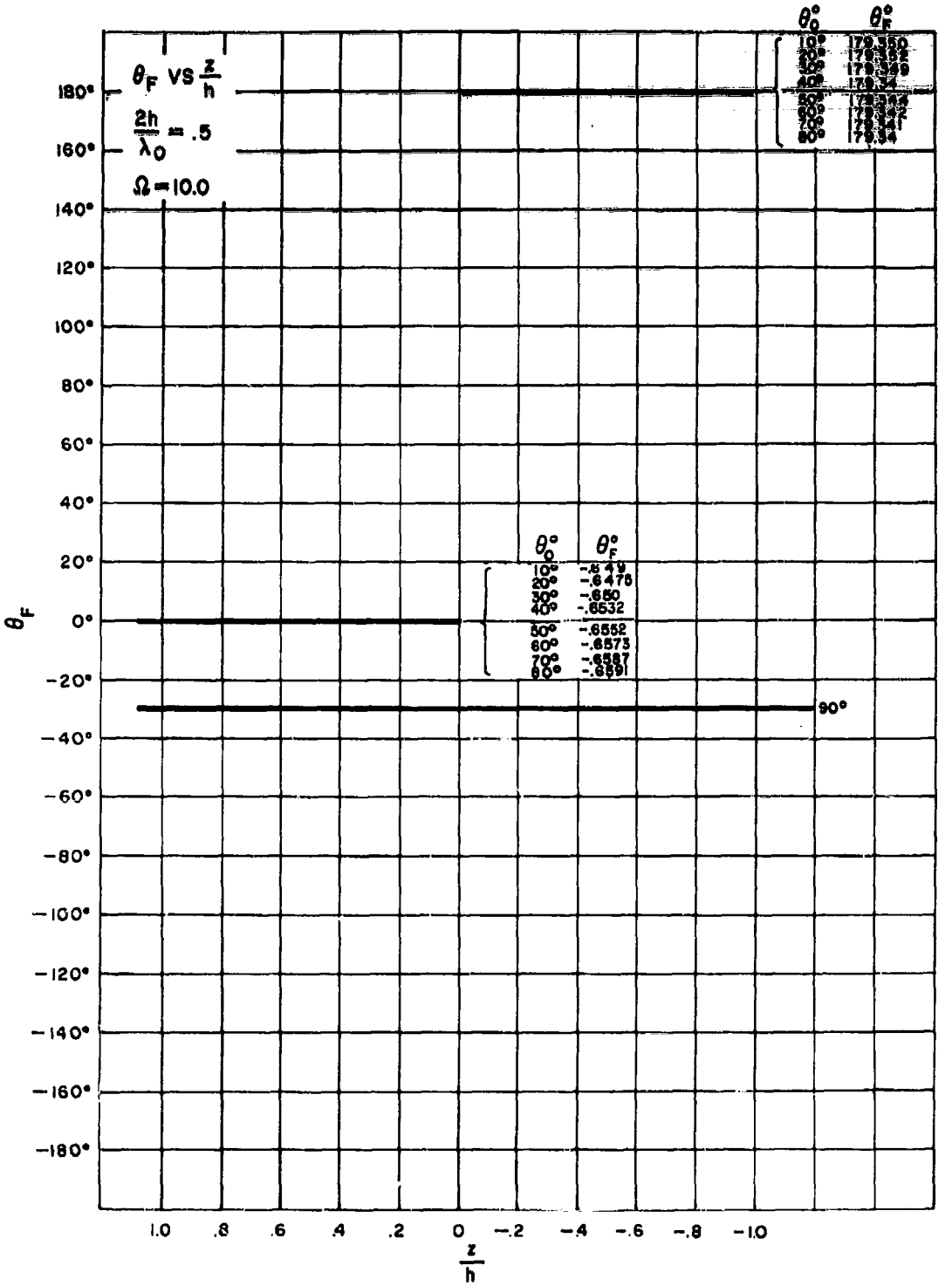

FIGURE 23. DISTRIBUTION OF "FORCED COMPONENT OF CURRENT"

$$I_F = |I_F| e^{j\theta_F}$$

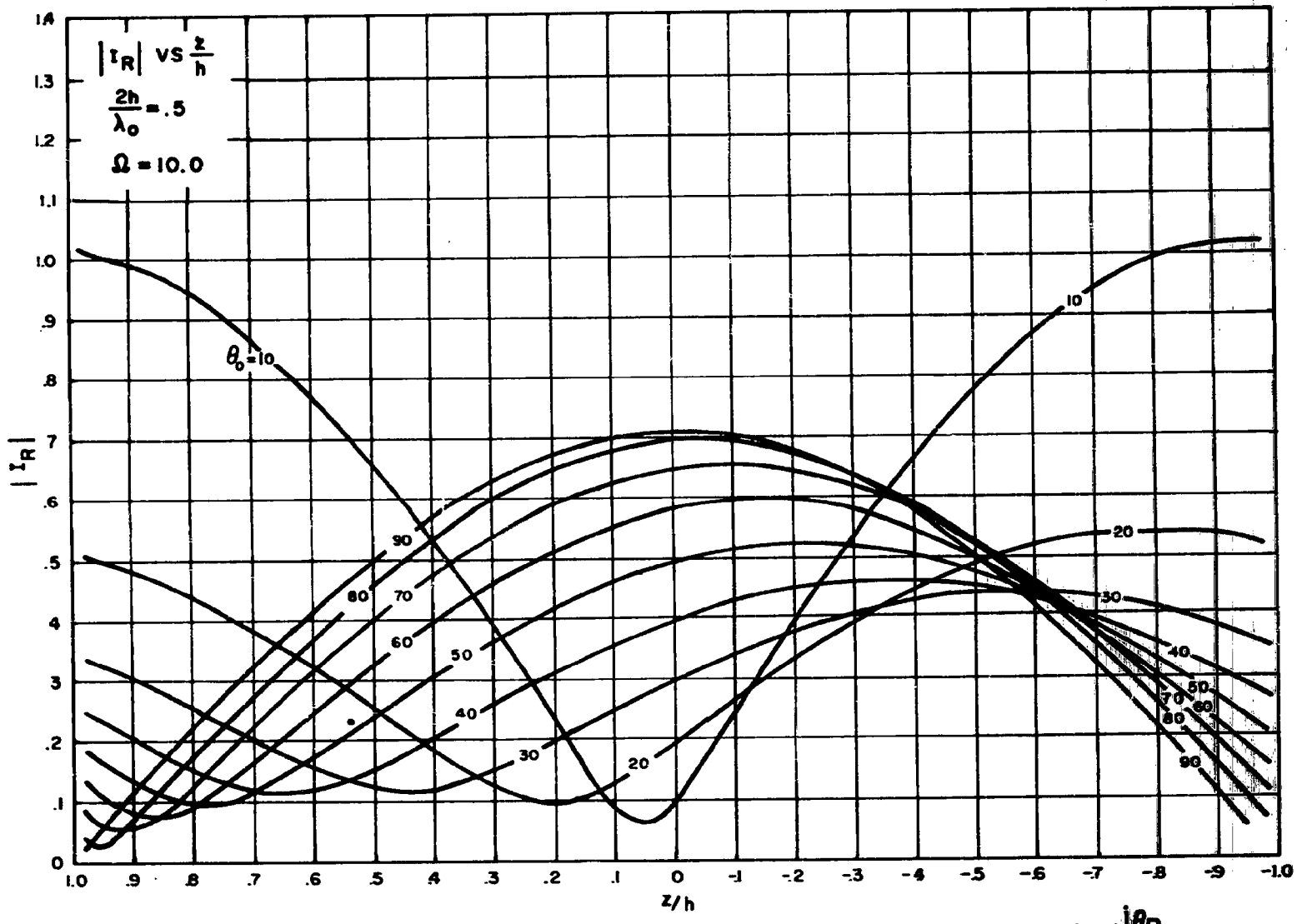

FIGURE 24. DISTRIBUTION OF "RESONANT COMPONENT OF CURRENT" $I_R = |I_R| e^{j\theta_R}$

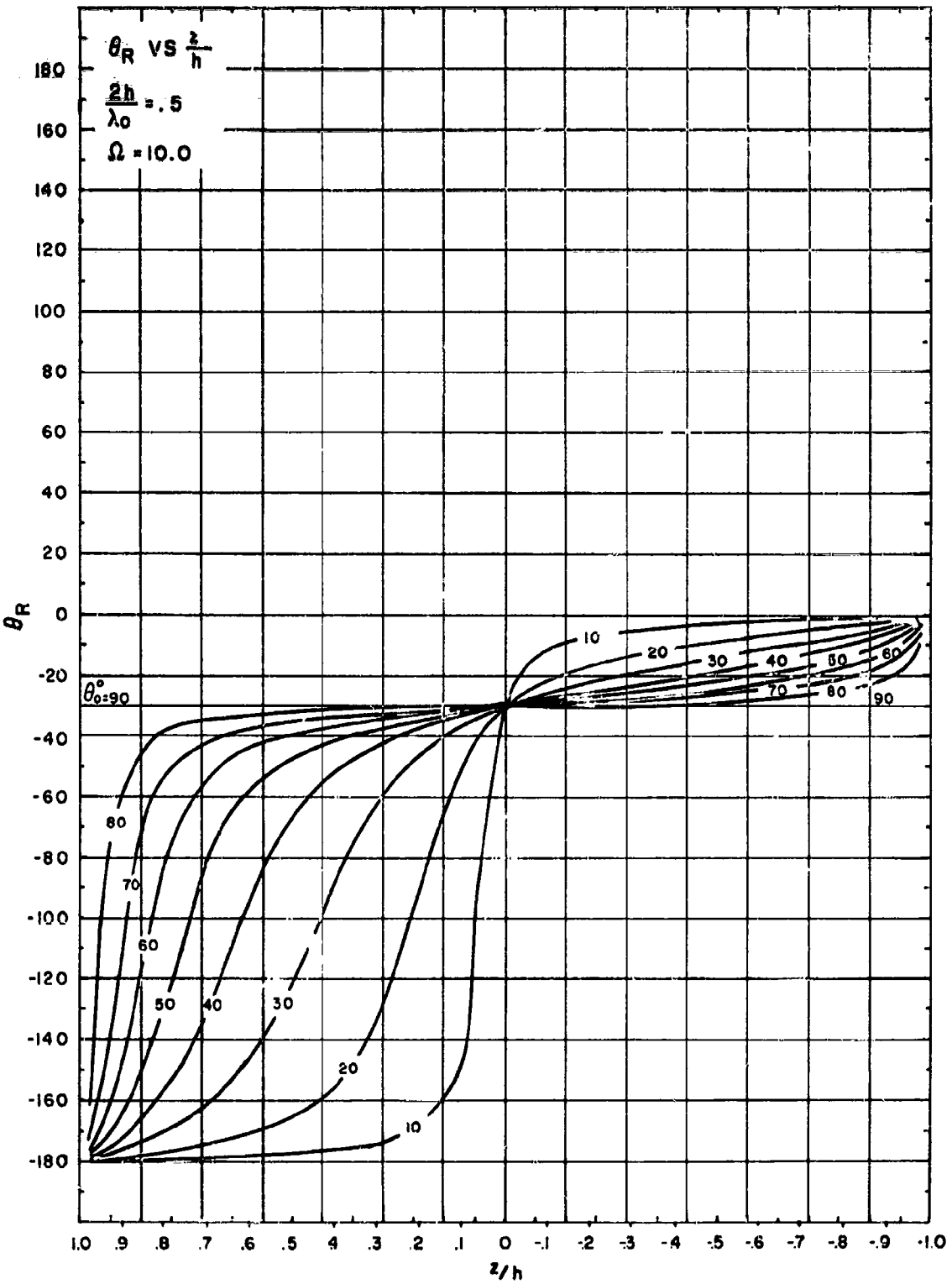

FIGURE 25. DISTRIBUTION OF "RESONANT COMPONENT OF CURRENT"
$I_R = |I_R| e^{j\theta_R}$

V. APPLICATION VIA TRANSMISSION EQUATION TO TRANSMISSION LOSSES

For bistatic cross section model measurements or in a system, an estimate of required receiver sensitivity can be obtained or an estimate of cross section calculated from the transmission equation.

A transmitter with average power P_T feeds a loss-less antenna of gain G_T located a distance R_T from the wire. A receiver is located a distance R_R from the wire and has a loss-less antenna of gain G_R. The gains G takes into account the polar diagrams of the antennas and are the values of gain in the direction of the wire. It is assumed that electric vector polarization of the transmitter is parallel to the incident plane, so that the incident polarization angle $\psi_T = 0$. Similarly, it is assumed that receiver polarization is parallel to the scattering or reflection plane containing the wire so that $\psi_R = 0$. The appropriate value of cross section to be used is $\sigma_{BS}(\theta_o, \theta)$ of the previous Section.

The received power will then be

$$P_R = \frac{P_T}{4\pi R_T^2} G_T \frac{\sigma}{4\pi R_R^2} \frac{G_R \lambda_o^2}{4\pi} \tag{27}$$

assuming that the load impedance of the receiver input is matched to the receiver antenna impedance. Writing losses as quantities such that losses in decibels will be positive, the total system loss is

$$L_T = \frac{P_T}{P_R} = \left(\frac{4\pi R_T^2}{\lambda_o}\right) \left(\frac{4\pi R_R}{\lambda_o}\right)^2 \frac{1}{(\sigma/\lambda_o^2)} \frac{1}{4\pi G_T G_R} \tag{28a}$$

$$= (L_o)_T (L_o)_R L_{sc} \frac{1}{G_T G_R} \tag{28b}$$

Equations (28a and 28b) are written in the form to allow use of the curves for σ/λ_o^2, where the free space losses

$$\left.\begin{aligned}(L_o)_T &= \left(\frac{4\pi R_T}{\lambda_o}\right)^2 \\ (L_o)_R &= \left(\frac{4\pi R_R}{\lambda_o}\right)^2\end{aligned}\right\} \qquad (29)$$

and the "scattering loss" L_{sc} is

$$L_{sc} = \frac{1}{(4\pi\sigma/\lambda_o^2)} \qquad (30)$$

In decibels

$$L_T(db) = L_{o_T}(db) + L_{o_R}(db) + L_{sc}(db) - G_T(db) - G_R(db) \qquad (31)$$

where the free space losses, in decibels, are given by

$$\begin{aligned}L_o(db) &= 36.56 + 20\log_{10}R(\text{miles}) + 20\log_{10}f(\text{mc/s}) \\ &= -23.43 + 20\log_{10}R(\text{miles}) + 20\log_{10}f(\text{kc/s}) \\ &= -27.56 + 20\log_{10}R(\text{meters}) + 20\log_{10}f(\text{mc/s}) \\ &= -87.56 + 20\log_{10}R(\text{meters}) + 20\log_{10}f(\text{kc/s})\end{aligned} \qquad (32)$$

and the "scattering loss" in decibels is

$$L_{sc}(db) = -10\log_{10}\left(\frac{4\pi\sigma}{\lambda_o^2}\right) \qquad (33)$$

The gains $G_T(db)$ and $G_R(db)$ are the antenna gains in decibels in the direction of the wire.

Putting (33) and (32) into (31) and using distances R in miles and frequencies in kc/s, (31) becomes

$$L_T(db) = -57.85 + 20 \log_{10} R_T(miles) + 20 \log_{10} R_R(miles) + 40 \log_{10} f(kc) - G_T(db) - G_R(db) - 10 \log_{10} \frac{\sigma}{\lambda_o^2} \quad (34)$$

As a special case, if $R_T = R_R = R$ and $G_T = G_R = G$

$$L_T(db) = -57.85 + 40 \log_{10} R \text{ (miles)} + 40 \log f(kc) - 2G(db) - 10 \log_{10} \frac{\sigma}{\lambda_o^2}$$

From (34), if distances, frequencies, antenna gains and L_{sc} are known total loss L_T can be computed which will give the required transmitter power for a given receiver power, by virtue of (28a), i.e.

$$P_T \text{ (dbw)} = P_R \text{ (dbw)} + L_T(db) \quad (35)$$

Conversely, if P_T and P_R are known so that L_T is known, and other parameters are known, then $L_{sc}(db)$ can be computed, viz (equation (34))

$$L_{sc}(db) = -10 \log_{10}\left(\frac{4\pi\sigma}{\lambda_o^2}\right) = L_T(db) + 46.86 - 20 \log_{10} R_T(miles) - 20 \log R_R(miles) - 40 \log_{10} f(kc) + G_T(db) + G_R(db) \quad (36)$$

Finally, the above has assumed that polarization angles $\psi_T = 0 = \psi_R$. For non-zero values of ψ, the received power in (27) will decrease, and (27) must be multiplied by $\cos^2 \psi_T \cos^2 \psi_R$. The total losses in (28) will increase by $1/(\cos^2 \psi_T \cos^2 \psi_R)$, or the loss $L_T(db)$ in (31) et seq. will increase by a polarization loss $L_p(db)$ given by

$$L_p(db) = -20 \left[\log \cos \psi_T + \log \cos \psi_R \right] \quad (37)$$

Consequently (31) is modified to take account of L_P and

$$L_T(db) = L_{o_T}(db) + L_{o_R}(db) + L_{sc}(db) + L_P(db) - G_R(db) - G_T(db) \qquad (38)$$

where $L_o(db)$ is given by (32), $L_{sc}(db)$ by (33) and $L_P(db)$ by (37).

As an example consider

$f = 100$ kc $\qquad R_T = R_R = 500$ miles $\qquad \psi_T = 60° = \psi_R$

$\frac{2h}{\lambda_o} = 1.0 \qquad \theta_o = 60°$

$\Omega = 10.0 \qquad \theta = 123°$

$G_T = G_R = 2.15$ db

From (32) $L_{o_T}(db) = L_{o_R}(db) = -23.43 + 53.98 + 40.00 = 60.55$ db. From Figure 15, for $\theta_o = 60°$, $\theta = 123°$, $\sigma / \lambda_o^2 = 1.14$ and L_{sc} -11.56 db. From (37) $L_P = -20\ (-.60206) = 12.04$ db. Hence, using (38)

$$L_T(db) = 121.10 - 11.56 + 12.04 - 4.30 = 117.28 \text{ db}$$

Hence a 10-watt transmitter ($P_T = 10$ dbw) would produce a received signal (matched receiver) of $10 - 117.28 = -107.28$ dbw or 1.871×10^{-11} watts. For a receiver resistance of 50 ohms the input voltage would be $-107.28 + 16.99 = -90.29$ db with respect to one volt or 29.71 db above one microvolt or about 30.6 microvolts.

VI. REFERENCES

1. Tai, C. T. "Radar Response from Thin Wires," Stanford Research Institute Report, Technical Rept. No. 18, March 1951.

2. King, R. W. P., "Linear Antennas," Chap. IV, Harvard U. Press, Cambridge, Mass. (1956).

3. Mentzer, J. R., "Scattering and Diffraction of Radio Waves," Pergamon Press, (1955).

4. King, R. W. P. and T. T. Wu, "The Scattering and Diffraction of Radio Waves," Harvard U. Press, Cambridge, Mass. (1959).

5. Cassedy, E. S., and J. Fainberg "Back Scattering Cross Sections of Cylindrical Wires," Trans. I. R. E., PGAP, Jan. 1960.

APPENDIX A

EVALUATION OF INTEGRALS USED IN SCATTERING COEFFICIENTS

A-I. INTRODUCTION

The purpose of this Appendix is to correct certain typographical errors in the evaluation of certain integrals employed in the variational method of Tai[1]. We shall employ here the notation of Tai. Let

$k = 2\pi / \lambda$ — θ = angle of incidence onto wire

$x = k\ell = 2\pi\ell/\lambda$ — ℓ = half length of wire

$q = \cos\theta$ — λ = free space wavelength

A-II. THE INTEGRAL g_c

$$g_c = k \sin\theta \int_{-\ell}^{\ell} f_c(z)\, e^{jkz\cos\theta}\, dz \qquad (I\text{-}1)$$

Using simple trigonometric identities, it can be shown that

$$g_c = \frac{4q\cos^2 qx \sin x - (1+q^2)\sin 2qx \cos x - 2q(1-q^2)\, x \cos x}{2q(1-q^2)^{1/2}} \qquad (I\text{-}2)$$

This is identical with Appendix A(2) of Tai[1].

A-III. THE INTEGRAL g_s

$$g_s = k \sin\theta \int_{-\ell}^{\ell} f_s(z)\, e^{jkz \cos\theta}\, dz \qquad (I\text{-}3)$$

$$= -j \frac{4q \sin^2 qz \cos z - (1+q^2) \sin 2qx \sin x + 2q(1-q^2)\, x \sin x}{2q(1-q^2)^{1/2}} \qquad (I\text{-}4)$$

This differs from Appendix A(3) of Tai[1] in the very last term of the numerator, where we find "sin x" instead of his "cos x."

In the above

$$\left.\begin{aligned} f_c(z) &= \cos qk\ell \cos kz - \cos qkz \cos k\ell \\ f_s(z) &= \sin qk\ell \sin kz - \sin qkz \sin k\ell \end{aligned}\right\} \qquad (I\text{-}5)$$

with

$$I_z = I_o \left[f_c(z) + A f_s(z) \right] \qquad (I\text{-}6)$$

is the trial current distribution, A and I_o being constants.

A-IV. THE Y_c INTEGRAL

$$Y_c = j \int_{-\ell}^{\ell} \int_{-\ell}^{\ell} f_c(z)\, f_c(z')\, K(z-z')\, dz\, dz' \qquad (I\text{-}7)$$

where the kernel is

$$K(z-z') = k\left(1 + \frac{1}{k^2} \frac{\partial^2}{\partial z^2} \frac{e^{-jkR}}{R}\right)$$

and

$$R = \left[(z-z')^2 + a^2\right]^{1/2}$$

Storer* has shown how integrals of this type may be evaluated by changing variable. The result is

$$Y_c = \cos^2 x \left[-1 + \cos 2x \cos 2qx + q \sin 2x \sin 2qx - j\,(\sin 2x \cos 2qx - q \cos 2x \sin 2qx)\right] - \frac{1}{2}\left[\frac{1+q^2}{q^2}\cos^2 x \cos 2qx + \sin 2x \sin 2qx\right]$$
$$\left[L(1+q)2x - L(1-q)2x\right] + j\left\{\cos^2 x\left[\frac{1+q^2}{q^2}\sin 2qx + (1-q^2)x\right]\right.$$
$$\left. - \cos^2 qx \sin 2x\right\}\left\{\log_e 4 + \Omega - L(1+q)2x - L(1-q)2x\right\}$$
$$+ \cos^2 qx\, L(4x) \qquad (I\text{-}8)$$

---

* Storer, J. E. "Variational Solution to the Problem of the Cylindrical Antenna," Doctoral Thesis, Harvard Univ., (1951).

A-V. THE Y_s INTEGRAL

We have

$$Y_s = j \int_{-\ell}^{\ell} \int_{-\ell}^{\ell} f_s(z)\, f_s(z')\, K(z-z')\, dz\, dz' \qquad (I\text{-}9)$$

and in a fashion like that for Y_c, this integral becomes

$$\begin{aligned} Y_s = \sin^2 x \Big[&-1 + \cos 2x \cos 2qx + q \sin 2x \sin 2qx \\ &-j(\sin 2x \cos 2qx - q \cos 2x \sin 2qx)\Big] + \frac{1}{2}\Big[\frac{1+q^2}{q^2}\sin^2 x \cos 2qx \\ &- \sin 2x \sin 2qx\Big] \Big[L(1+q)2x - L(1-q)2x\Big] \qquad (I\text{-}10) \\ &+ j\Big\{-\sin^2 x\Big[\frac{1+q^2}{q^2}\sin 2qx - (1-q^2)x\Big] + \sin^2 qx \sin 2x\Big\} \\ &\Big\{\log_e 4 + \Omega - L(1+q)2x - L(1-q)2x\Big\} + \sin^2 qx\, L(4x) \end{aligned}$$

In the Y-integrals above, the evaluations assume that the wire is thin, i.e. $\ell >> a$. The L-functions are tabulated functions, given by sine and cosine integrals.

$$L(1 \pm q)2p = \int_0^{(1\pm q)2p} \frac{1-e^{-ju}}{u}\, du = \mathrm{Cin}(1+q)2p + jSi(1+q)2p \qquad (I\text{-}11)$$

The Y_c-integrals (I-8) differ from that of Appendix A(6) of Tai in that a term $\cos^2 qx\, L(4x)$ was omitted from the latter. Similarly in the Y_s-integral (I-10), a term $\sin^2 qx L(4x)$ was omitted from Tai's expression in his Appendix A(7).

With the above corrections, the expressions in the text for g_c, g_s, Y_c and Y_s were used with the evaluations of (I-2), (I-4), (I-8) and (I-10).

UNCLASSIFIED

UNCLASSIFIED